

Persistent coding of outcome-predictive cue features in the rat nucleus accumbens.

Authors: Jimmie M. Gmaz¹, James E. Carmichael¹, Matthijs A. A. van der Meer^{1*}

¹Department of Psychological and Brain Sciences, Dartmouth College, Hanover NH 03755

*Correspondence should be addressed to MvdM, Department of Psychological and Brain Sciences, Dartmouth College, 3 Maynard St, Hanover, NH 03755. E-mail: mvdm@dartmouth.edu.

Acknowledgments: We thank Nancy Gibson, Martin Ryan and Jean Flanagan for animal care, and Min-Ching Kuo and Alyssa Carey for technical assistance. This work was supported by Dartmouth College (Dartmouth Fellowship to JMG and JEC, and start-up funds to MvdM) and the Natural Sciences and Engineering Research Council (NSERC) of Canada (Discovery Grant award to MvdM, Canada Graduate Scholarship to JMG).

Conflict of Interest: The authors declare no competing financial interests.

1 Abstract

2 The nucleus accumbens (NAc) is important for learning from feedback and for biasing and invigorating
3 behavior in response to cues that predict motivationally relevant outcomes. NAc encodes outcome-related
4 cue features such as the magnitude and identity of reward. However, little is known about how features
5 of cues themselves are encoded. We designed a decision making task where rats learned multiple sets of
6 outcome-predictive cues, and recorded single-unit activity in the NAc during performance. We found that
7 coding of various cue features occurred alongside coding of expected outcome. Furthermore, this coding
8 persisted both during a delay period, after the rat made a decision and was waiting for an outcome, and
9 after the outcome was revealed. Encoding of cue features in the NAc may enable contextual modulation
10 of ongoing behavior, and provide an eligibility trace of outcome-predictive stimuli for updating stimulus-
11 outcome associations to inform future behavior.

12 Introduction

13 Theories of nucleus accumbens (NAc) function generally agree that this brain structure contributes to moti-
14 vated behavior, with some emphasizing a role in learning from reward prediction errors (RPEs) (Averbeck &
15 Costa 2017; Joel, Niv, & Ruppin 2002; Khamassi & Humphries 2012; Lee, Seo, & Jung 2012; Maia 2009;
16 Schultz 2016; see also the addiction literature on effects of drug rewards; Carelli 2010; Hyman, Malenka,
17 & Nestler 2006; Kalivas & Volkow 2005) and others a role in the modulation of ongoing behavior through
18 stimuli associated with motivationally relevant outcomes (invigorating, directing; Floresco, 2015; Nicola,
19 2010; Salamone & Correa, 2012). These proposals echo similar ideas on the functions of the neuromod-
20 ulator dopamine (Berridge, 2012; Maia, 2009; Salamone & Correa, 2012; Schultz, 2016), with which the
21 NAc is tightly linked functionally as well as anatomically (Cheer et al., 2007; du Hoffmann & Nicola, 2014;
22 Ikemoto, 2007; Takahashi, Langdon, Niv, & Schoenbaum, 2016).

23 Much of our understanding of NAc function comes from studies of how cues that predict motivationally rel-
24 evant outcomes (e.g. reward) influence behavior and neural activity in the NAc. Task designs that associate
25 such cues with rewarding outcomes provide a convenient access point eliciting conditioned responses such as
26 sign-tracking and goal-tracking (Hearst & Jenkins, 1974; Robinson & Flagel, 2009), pavlovian-instrumental
27 transfer (Estes, 1943; Rescorla & Solomon, 1967) and enhanced response vigor (Nicola, 2010; Niv, Daw,
28 Joel, & Dayan, 2007), which tend to be affected by NAc manipulations (Chang, Wheeler, & Holland 2012;
29 Corbit & Balleine 2011; Flagel et al. 2011; although not always straightforwardly; Chang & Holland 2013;
30 Giertler, Bohn, & Hauber 2004). Similarly, analysis of RPEs typically proceeds by establishing an associa-
31 tion between a cue and subsequent reward, with NAc responses transferring from outcome to the cue with
32 learning (Day, Roitman, Wightman, & Carelli, 2007; Roitman, Wheeler, & Carelli, 2005; Schultz, Dayan, &
33 Montague, 1997; Setlow, Schoenbaum, & Gallagher, 2003).

34 Surprisingly, although substantial work has been done on the coding of outcomes predicted by such cues
35 (Atallah, McCool, Howe, & Graybiel, 2014; Bissonette et al., 2013; Cooch et al., 2015; Cromwell & Schultz,

36 2003; Day, Wheeler, Roitman, & Carelli, 2006; Goldstein et al., 2012; Hassani, Cromwell, & Schultz, 2001;
37 Hollerman, Tremblay, & Schultz, 1998; Lansink et al., 2012; McGinty, Lardeux, Taha, Kim, & Nicola,
38 2013; Nicola, 2004; Roesch, Singh, Brown, Mullins, & Schoenbaum, 2009; Roitman et al., 2005; Saddoris,
39 Stamatakis, & Carelli, 2011; Schultz, Apicella, Scarnati, & Ljungberg, 1992; Setlow et al., 2003; Sugam,
40 Saddoris, & Carelli, 2014; West & Carelli, 2016), much less is known about how outcome-predictive cues
41 themselves are encoded in the NAc (but see; Sleezer, Castagno, & Hayden, 2016). This is an important issue
42 for at least two reasons. First, in reinforcement learning, motivationally relevant outcomes are typically
43 temporally delayed relative to the cues that predict them. In order to solve the problem of assigning credit
44 (or blame) across such temporal gaps, some trace of preceding activity needs to be maintained (Lee et al.,
45 2012; Sutton & Barto, 1998). For example, if you become ill after eating food X in restaurant A, depending
46 on if you remember the identity of the restaurant or the food at the time of illness, you may learn to avoid
47 all restaurants, restaurant A only, food X only, or the specific pairing of X-in-A. Therefore, a complete
48 understanding of what is learned following feedback requires understanding what trace is maintained. Since
49 NAc is a primary target of DA signals interpretable as RPEs, and NAc lesions impair RPEs related to timing,
50 its activity trace will help determine what can be learned when RPEs arrive (Hamid et al., 2015; Hart,
51 Rutledge, Glimcher, & Phillips, 2014; Ikemoto, 2007; McDannald, Lucantonio, Burke, Niv, & Schoenbaum,
52 2011; Takahashi et al., 2016). Similarly, in a neuroeconomics framework, NAc is thought to represent a
53 domain-general subjective value associated with different offers (Bartra, McGuire, & Kable, 2013; Levy &
54 Glimcher, 2012; Peters & Büchel, 2009; Sescousse, Li, & Dreher, 2015); representation of the offer itself
55 would provide a potential means for updating offer value.

56 Second, for ongoing behavior, the relevance of cues typically depends on context. In experimental set-
57 tings, context may include the identity of a preceding cue, spatial or configural arrangements (Bouton, 1993;
58 Holland, 1992; Honey, Iordanova, & Good, 2014), and unsignaled rules as occurs in set shifting and other
59 cognitive control tasks (Cohen & Servan-Schreiber, 1992; Floresco, Ghods-Sharifi, Vexelman, & Magyar,
60 2006; Grant & Berg, 1948; Sleezer et al., 2016). In such situations, the question arises how selective, context-
61 dependent processing of outcome-predictive cues is implemented. For instance, is there a gate prior to NAc

62 such that only currently relevant cues are encoded in NAc, or are all cues represented in NAc but their current
63 values dynamically updated (FitzGerald, Schwartenbeck, & Dolan, 2014; Goto & Grace, 2008; Sleezer et
64 al., 2016). Representation of cue identity would allow for context-dependent mapping of outcomes predicted
65 by specific cues.

66 Thus, both from a learning and a flexible performance perspective, it is of interest to determine how cue
67 identity is represented in the brain, with NAc of particular interest given its anatomical and functional po-
68 sition at the center of motivational systems. We sought to determine whether cue identity is represented in
69 the NAc, if cue identity is represented alongside other motivationally relevant variables, such as cue value,
70 and if these representations are maintained after a behavioral decision has been made (Figure 1). To address
71 these questions, we recorded the activity of NAc units as rats performed a task in which multiple, distinct
72 sets of cues predicted the same outcome.

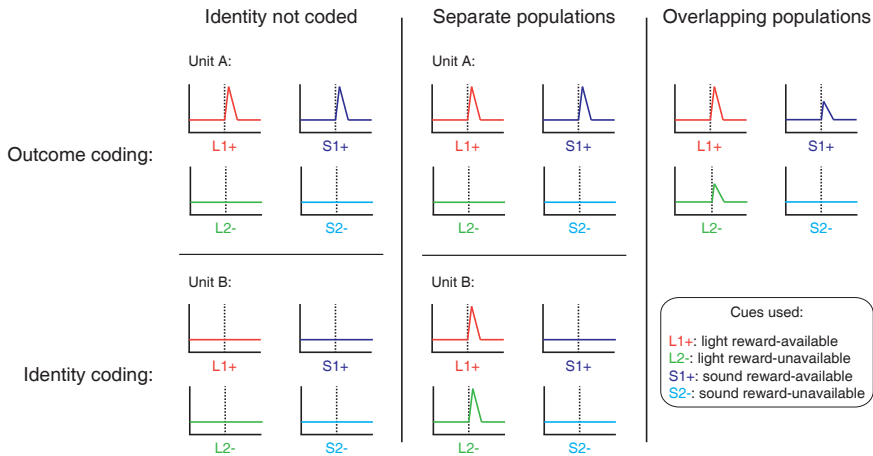
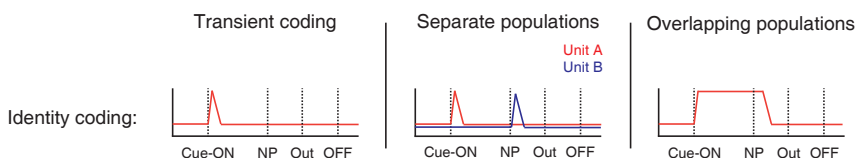
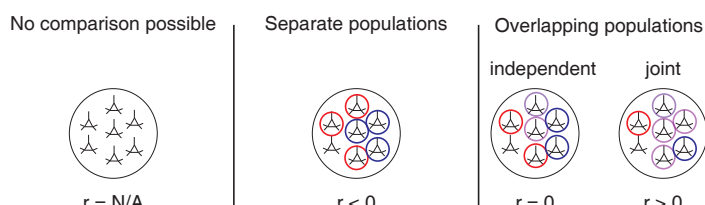
A**Presence of cue feature coding****B****Persistence of cue feature coding****C****Quantification of coding across units and time epochs**

Figure 1: Schematic of potential coding strategies for cue feature coding employed by single units in the NAc across different cue features (A) and phases of a trial (B). **A:** Displayed are schematic PETHs illustrating putative responses to different cues under different hypotheses of how cue identity (light, sound) and outcome (reward-available, reward-unavailable) are coded. Left panel: Coding of identity is absent in the NAc. Top: Unit A encodes a motivationally relevant variable, such as expected outcome, similarly across other cue features, such as identity or physical location. Hypothetical plot is firing rate across time. L1+ (red) signifies a reward-available light cue, S1+ (navy blue) a reward-available sound cue, L2- (green) a reward-unavailable light cue, S2- (light blue) a reward-unavailable sound cue. Dashed line indicates onset of cue. Bottom: No units within the NAc discriminate their firing according to cue identity. Middle panel: Coding of identity occurs in a separate population of units from encoding of other cue features such as expected outcome or physical location. Top: Same as left panel, with unit A discriminating between reward-available and reward-unavailable cues. Bottom: Unit B discriminates firing across stimulus modalities, depicted here as firing to light cues but not sound cues. Right panel: Coding of identity occurs in an overlapping population of cells with coding of other motivationally relevant variables. Hypothetical example demonstrating a unit that responds to reward-predictive cues, but firing rate is also modulated by the stimulus modality of the cue, firing most for the reward-available light cue. **B:** Displayed are schematic PETHs illustrating potential ways in which identity coding may persist over time. Left panel: Cue-onset triggers a transient response to a unit that codes for cue identity. Dashed lines indicate time of a behavioral or environmental event. 'Cue-ON' signifies onset of cue, 'NP' signifies when the rat holds a nosepoke at a reward receptacle, 'Out' signifies when the outcome is revealed, 'OFF' signifies when the cue turns off. Middle and right panel: Identity coding persists at other time points, shown here during a nosepoke hold period until outcome is revealed. Coding can either be maintained by a sequence of units (middle panel) or by the same unit as during cue-onset (right panel).

Figure 1: (Previous page.) **C:** Schematic pool of NAc units, illustrating the different possible outcomes for each of the analyses. R values represent the correlation between sets of recoded regression coefficients (see text for analysis details). Left panel: Cue identity is not coded (A: left panel), or is only transiently represented in response to the cue (B: left panel). Middle panel: Negative correlation ($r < 0$) suggests that identity and outcome coding are represented by separate populations of units (A: middle panel), or identity coding is represented by distinct units among different points in a trial (B: middle panel). Red circles represents coding for one cue feature or point in time, blue circles for the other cue feature or point in time. Right panel: Identity and outcome coding (A: right panel), or identity coding at cue-onset and nosepoke (B: right panel) are represented by overlapping populations of units, shown here by the purple circles. The absence of a correlation ($r \sim 0$) suggests that the overlap of identity and outcome coding, or cue-onset and nosepoke coding, is expected by chance and that the two cue features, or points in time, are coded independently from one another. A positive correlation ($r > 0$) implies a higher overlap than expected by chance, suggesting joint coding. Note: The same hypotheses apply to other aspects of the environment when the cue is presented, such as the physical location of the cue, as well as other time epochs within the task, such as when the animal receives feedback about an approach.

73 Results

74 Behavior

75 Rats were trained to discriminate between cues signaling the availability and absence of reward on a square
76 track with four identical arms for two distinct set of cues (Figure 2). During each session, rats were pre-
77 sented sequentially with two behavioral blocks containing cues from different sensory modalities, a light and
78 a sound block, with each block containing a cue that signalled the availability of reward (reward-available),
79 and a cue that signalled the absence of reward (reward-unavailable). To maximize reward receipt, rats should
80 approach reward sites on reward-available trials, and skip reward sites on reward-unavailable trials (see Fig-
81 ure 3A for an example learning curve). All four rats learned to discriminate between the reward-available
82 and reward-unavailable cues for both the light and sound blocks as determined by reaching significance ($p <$
83 .05) on a daily chi-square test comparing approach behavior for reward-available and reward-unavailable
84 cues for each block, for at least three consecutive days (range for time to criterion: 22 - 57 days). Mainte-
85 nance of behavioral performance during recording sessions was assessed using linear mixed effects models
86 for both proportion of trials where the rat approached the receptacle, and trial length. Analyses revealed
87 that the likelihood of a rat to make an approach was influenced by whether a reward-available or reward-

88 unavailable cue was presented, but was not significantly modulated by whether the rat was presented with a
89 light or sound cue (Percentage approached: light reward-available = 97%; light reward-unavailable = 34%;
90 sound reward-available = 91%; sound reward-unavailable 35%; cue identity $p = .115$; cue outcome $p < .001$;
91 Figure 3B). A similar trend was seen with the length of time taken to complete a trial (Trial length: light
92 reward-available = 1.85 s; light reward-unavailable = 1.74 s; sound reward-available = 1.91 s; sound reward-
93 unavailable 1.78 s; cue identity $p = .106$; cue outcome $p < .001$; Figure 3C). Thus, during recording, rats
94 successfully discriminated the cues according to whether or not they signaled the availability of reward at
95 the reward receptacle.

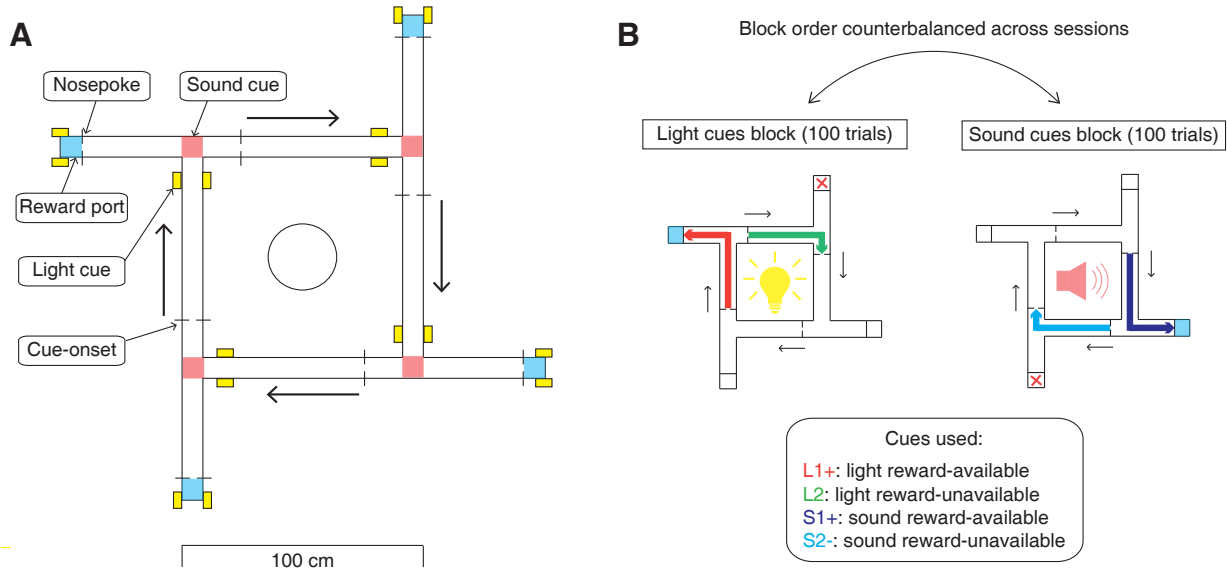


Figure 2: Schematic of behavioral task. **A:** To scale depiction of square track consisting of multiple identical T-choice points. At each choice point, the availability of 12% sucrose reward at the nearest reward receptacle (light blue fill) was signaled by one of four possible cues, presented when the rat initiated a trial by crossing a photobeam on the track (dashed lines). Photobeams at the ends of the arms by the receptacles registered Nosepokes (solid lines). Rectangular boxes with yellow fill indicate location of LEDs used for light cues. Speakers for sound cues were placed underneath the choice points, indicated by magenta fill on track. Arrows outside of track indicate correct running direction. Circle in the center indicates location of pedestal during pre- and post-records. Scale bar is located beneath the track. **B:** Progression of a recording session. A session was started with a 5 minute recording period on a pedestal placed in the center of the apparatus. Rats then performed the light and sound blocks of the cue discrimination task in succession for 100 trials each, followed by another 5 minute recording period on the pedestal. Left in figure depicts a light block, showing an example trajectory for a correct reward-available (approach trial; red) and reward-unavailable (skip trial; green) trial. Right in figure depicts a sound block, with a reward-available (approach trial; navy blue) and reward-unavailable (skip trial; light blue) trial. Ordering of the light and sound blocks was counterbalanced across sessions. Reward-available and reward-unavailable cues were presented pseudo-randomly, such that not more than two of the same type of cue could be presented in a row. Location of the cue on the track was irrelevant for behavior, all cue locations contained an equal amount of reward-available and reward-unavailable trials.

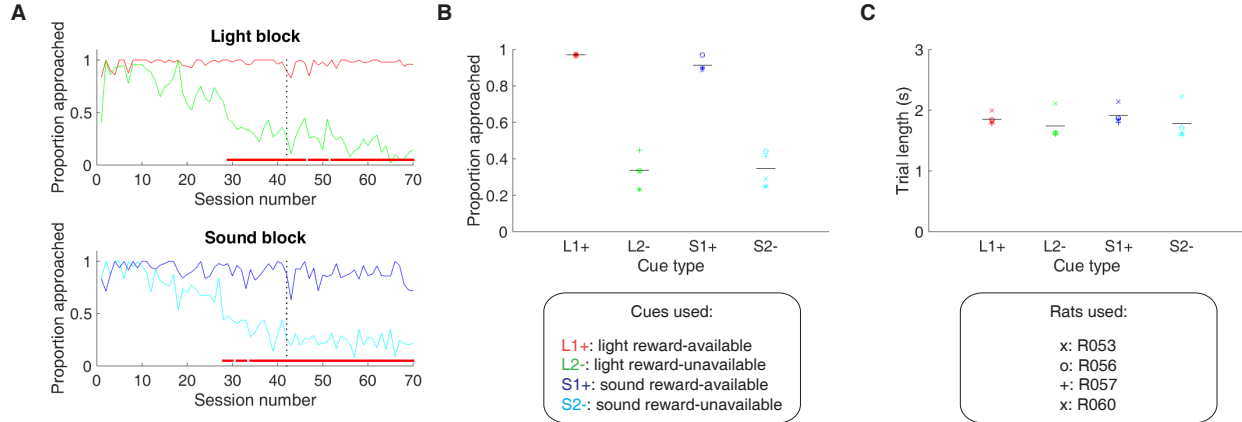


Figure 3: Performance on the behavioral task. **A.** Example learning curves across sessions from a single subject (R060) showing the proportion approached for reward-available (red line for light block, navy blue line for sound block) and reward-unavailable trials (green line for light block, light blue line for sound block) for light (top) and sound (bottom) blocks. Fully correct performance corresponds to an approach proportion of 1 for reward-available trials and 0 for reward-unavailable trials. Rats initially approach on both reward-available and reward-unavailable trials, and learn with experience to skip non-rewarded trials. Red bars indicate days in which a rat statistically discriminated between reward-available and reward-unavailable cues, determined by a chi square test. Dashed line indicates time of electrode implant surgery. **B-C:** Summary of performance during recording sessions for each rat. **B:** Proportion approached for all rats, averaged across all recording sessions. Different columns indicate the different cues (reward-available (red) and reward-unavailable (green) light cues, reward-available (navy blue) and reward-unavailable (light blue) sound cues). Different symbols correspond to individual subjects; horizontal black line shows the mean. All rats learned to discriminate between reward-available and reward-unavailable cues, as indicated by the clear difference of proportion approached between reward-available (~90% approached) and reward-unavailable cues (~30% approached), for both blocks (see Results for statistics). **C:** Average trial length for each cue. Note that the time to complete a trial was comparable for the different cues.

96 NAc encodes behaviorally relevant and irrelevant cue features

97 We sought to address which parameters of our task were encoded by NAc activity, specifically whether
98 the NAc encodes aspects of motivationally relevant cues not directly tied to reward, such as the identity
99 and location of the cue, and whether this coding is accomplished by separate or overlapping populations
100 (Figure 1A). To do this we recorded a total of 443 units with > 200 spikes in the NAc from 4 rats over 57
101 sessions (range: 12 - 18 sessions per rat) while they performed a cue discrimination task (Table 1). Units that
102 exhibited a drift in firing rate over the course of either block, as measured by a Mann-Whitney U comparing
103 firing rates for the first and second half of trials within a block, were excluded from further analysis, leaving
104 344 units for further analysis. The activity of 133 (39%) of these 344 units were modulated by the cue, with
105 more showing a decrease in firing ($n = 103$) than an increase ($n = 30$) around the time of cue-onset (Table 1).
106 Within this group, 24 were classified as FSIs, while 109 were classified as SPNs. Upon visual inspection, we
107 observed several patterns of firing activity, including units that discriminated firing upon cue-onset across
108 various cue conditions, showed sustained differences in firing across cue conditions, had transient responses
109 to the cue, showed a ramping of activity starting at cue-onset, and showed elevated activity immediately
110 preceding cue-onset (Figure 4).

111 To characterize more formally whether these cue-evoked responses were modulated by various aspects of
112 the task, we fit a forward selection stepwise generalized linear model (GLM) to each cue-modulated unit for
113 1 second post cue-onset. Fitting GLMs to all trials within a session revealed that a variety of task parameters
114 accounted for a significant portion of firing rate variance in NAc cue-modulated units (Figure 5A-B,??, Table
115 1). Notably, there were units that discriminated between the light or sound block (28% of cue-modulated
116 units, accounting for 6% of variance on average), between arms of the maze (38% of cue-modulated units,
117 accounting for 6% of variance on average), and between the common portion of reward-available or reward-
118 unavailable trials (26% of cue-modulated units, accounting for 4% of variance on average), suggesting that
119 the NAc encodes features of reward-predictive cues in addition to expected outcome (Figure 4,??,??,??).

120 **UPDATE SECTION: To determine whether overlap of coding of cue features was different than ex-**

121 pected by chance we correlated recoded beta coefficients from the GLMs (Figure 5D). This revealed
122 that cue identity was coded independently from both cue outcome ($r = -.018$; $p = .840$) and cue loca-
123 tion ($r = .107$; $p = .220$), as determined by non-significant correlations, but that cue location and cue
124 outcome were encoded jointly ($r = .221$; $p = .011$), as signified by a significant positive correlation.
125 Chi-square tests depicted a similar pattern of results (cue identity and cue location = $\chi = .687$, $p =$
126 $.407$; cue identity and cue outcome = $\chi = .022$, $p = .882$; cue location and cue outcome = $\chi = 3.02$, p
127 = $.082$). The GLM fitting was repeated for the first half of the trials in each stimulus block. This revealed
128 a qualitatively similar pattern of results, suggesting that this selectivity is present early within a block (first
129 half of block vs. all trials: 37 vs. 37, 45 vs. 50, and 25 vs. 34 units for cue identity, cue location, and cue
130 outcome, respectively). To control for differences that may have arisen do to different behavior at the choice
131 point, we also analyzed our data for approach trials only. Comparison of the GLMs using only approach
132 trials versus all trials was qualitatively similar (approach trials vs. all trials: 33 vs. 37, 45 vs. 50, and 28 vs.
133 34 units for cue identity, cue location, and cue outcome, respectively). Additionally, a sliding window GLM
134 centered on cue-onset revealed that cue identity and cue location contributed to the activity of a significant
135 proportion of cue-modulated units throughout this epoch, whereas an increase in units encoding cue outcome
136 became apparent after cue-onset (z -score > 1.96 when comparing proportion of units to that observed when
137 shuffling the firing rates before running the GLM, Figure 5D). Together, these findings show that various cue
138 features are represented in the NAc in overlapping populations, that cue modality is coded independently
139 from cue outcome and cue location, and that cue outcome and cue location are coded jointly (Figure 1).

Task parameter	Total	↑ MSN	↓ MSN	↑ FSI	↓ FSI
All units	443	155	216	27	45
<i>Rat ID</i>					
R053	145	51	79	4	11
R056	70	12	13	17	28
R057	136	55	75	3	3
R060	92	37	49	3	3
Analyzed units	344	117	175	18	34
Cue modulated units	133	24	85	6	18
<i>GLM aligned to cue-onset</i>					
Cue identity	42 (28%)	7 (29%)	21 (25%)	1 (17%)	8 (44%)
Cue location	55 (38%)	13 (54%)	27 (32%)	3 (50%)	7 (39%)
Cue outcome	26 (26%)	10 (42%)	18 (21%)	0 (-)	6 (33%)
Approach behavior	32 (23%)	8 (33%)	18 (21%)	1 (17%)	4 (22%)
Trial length	22 (19%)	5 (21%)	18 (21%)	0 (-)	2 (11%)
Trial number	42 (24%)	11 (46%)	12 (14%)	1 (17%)	8 (44%)
Previous trial	8 (4%)	0 (-)	5 (6%)	0 (-)	0 (-)
<i>GLM aligned to nosepoke</i>					
Cue identity	28 (50%)	14 (58%)	36 (42%)	2 (33%)	14 (78%)
Cue location	30 (50%)	14 (58%)	40 (47%)	3 (50%)	9 (50%)
Cue outcome	23 (32%)	8 (33%)	29 (34%)	0 (-)	5 (28%)
<i>GLM aligned to outcome</i>					
Cue identity	25 (8%)	0 (-)	6 (7%)	0 (-)	4 (22%)
Cue location	31 (8%)	0 (-)	6 (7%)	0 (-)	4 (22%)
Cue outcome	34 (8%)	0 (-)	6 (7%)	0 (-)	4 (22%)

Table 1: Overview of recorded NAc units and their relationship to task variables at various time epochs. Percentage is relative to the number of cue-modulated units (n = 133).

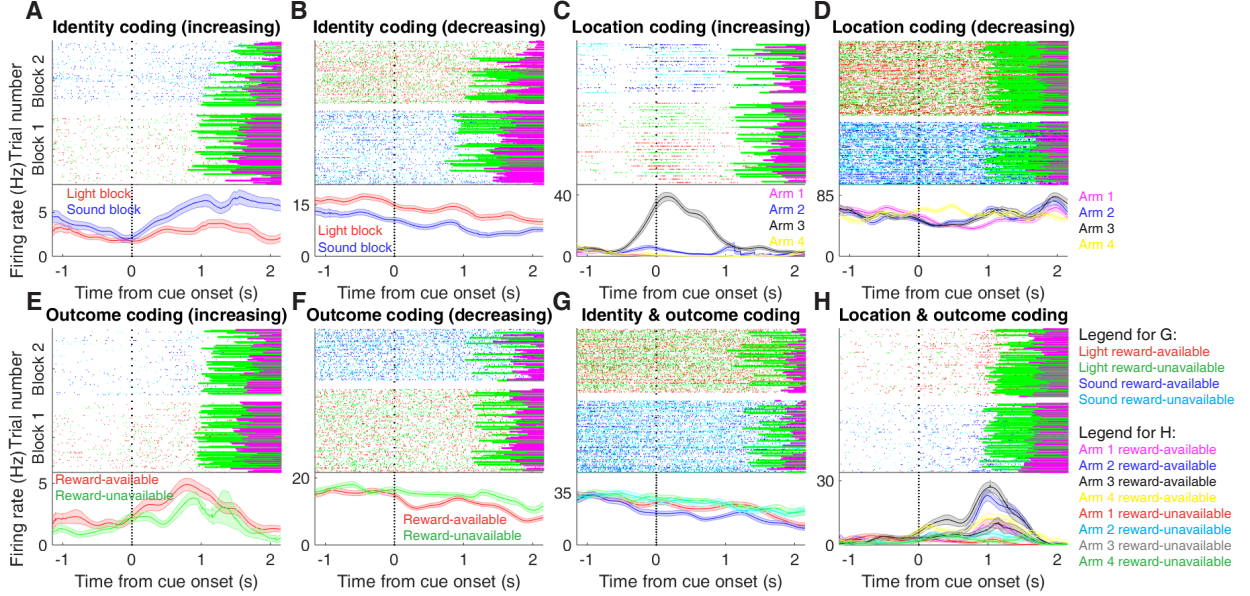


Figure 4: Examples of cue-modulated NAc units influenced by different task parameters. **A:** Example of a cue-modulated NAc unit that showed an increase in firing following the cue, and exhibited identity coding. Top: rasterplot showing the spiking activity across all trials aligned to cue-onset. Spikes across trials are color-coded according to cue type (red: reward-available light; green: reward-unavailable light; navy blue: reward-available sound; light blue: reward-unavailable sound). Green and magenta bars indicate trial termination when a rat initiated the next trial or made a nosepoke, respectively. White space halfway up the rasterplot indicates switching from one block to the next. Dashed line indicates cue-onset. Bottom: PETHs showing the average smoothed firing rate for the unit for trials during light (red) and sound (blue) blocks, aligned to cue-onset. Lightly shaded area indicates standard error of the mean. Note this unit showed a larger increase in firing to sound cues. **B:** An example of a unit that was responsive to cue identity as in A, but for a unit that showed a decrease in firing to the cue. Note the sustained higher firing rate during the light block. **C-D:** Cue-modulated units that exhibited location coding, each color in the PETHs represents average firing response for a different cue location. **C:** The firing rate of this unit only changed on arm 3 of the task. **D:** Firing decreased for this unit on all arms but arm 4. **E-F:** Cue-modulated units that exhibited outcome coding, with the PETHs comparing reward-available (red) and reward-unavailable (green) trials. **E:** This unit showed a slightly higher response during presentation of reward-available cues. **F:** This unit showed a dip in firing when presented with reward-available cues. **G-H:** Examples of cue-modulated units that encoded multiple cue features. **G:** This unit showed both identity and outcome coding. **H:** An example of a unit that coded for both identity and location.

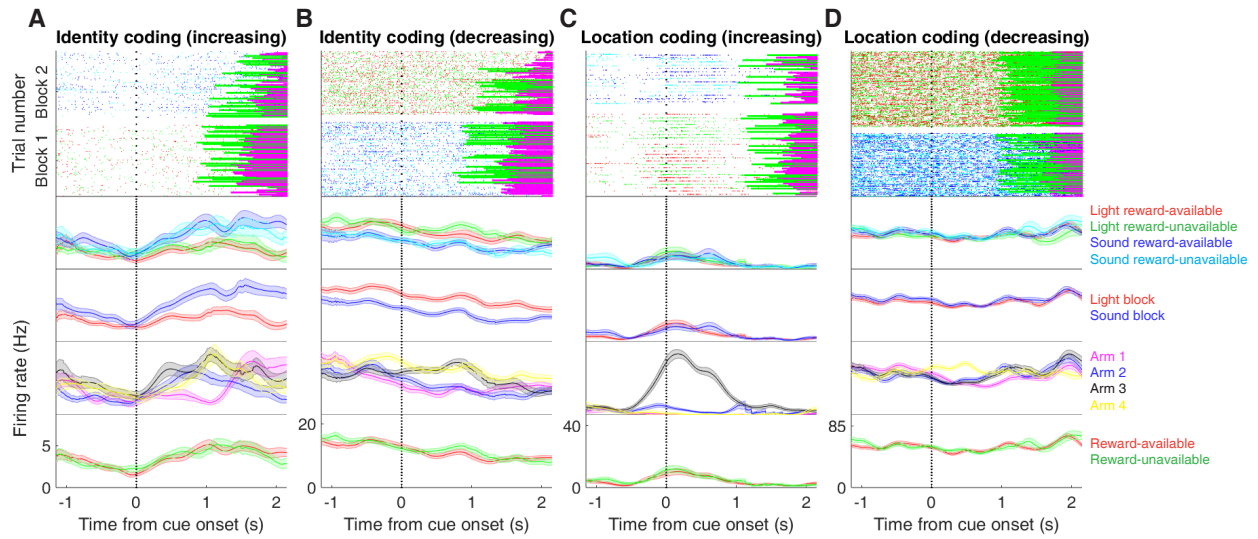


Figure supplement 1 Expanded examples of cue-modulated NAc units influenced by different task parameters for Figure 4A-D, showing firing rate breakdown by: cue type (top PETH), cue identity (top-middle PETH), cue location (bottom-middle PETH), and cue outcome (bottom PETH).

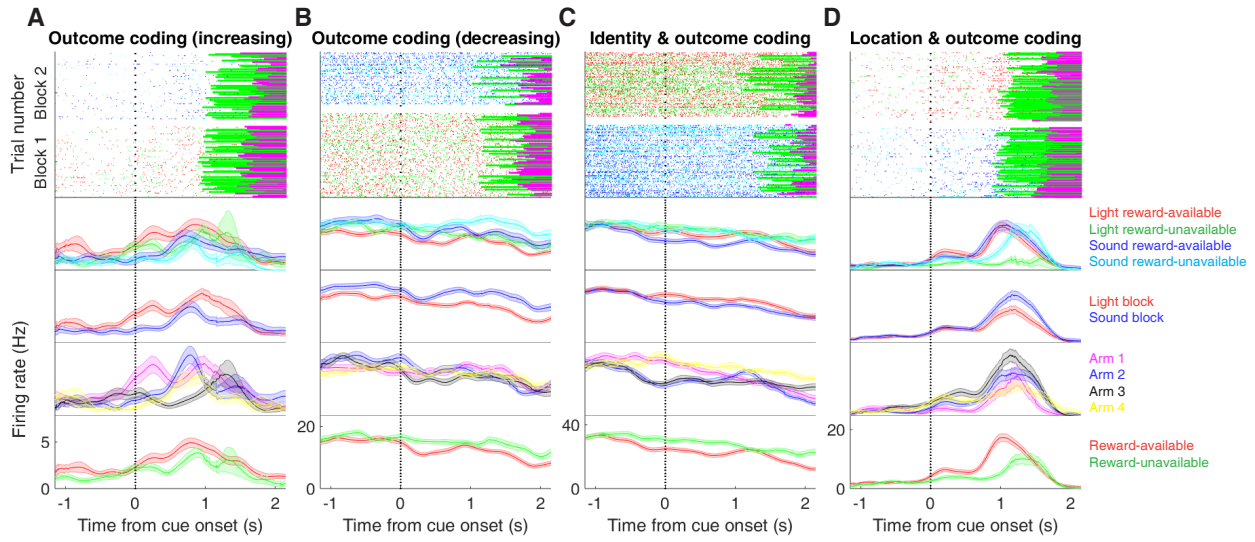


Figure supplement 2 Expanded examples of cue-modulated NAc units influenced by different task parameters for Figure 4E-H, showing firing rate breakdown by: cue type (top PETH), cue identity (top-middle PETH), cue location (bottom-middle PETH), and cue outcome (bottom PETH).

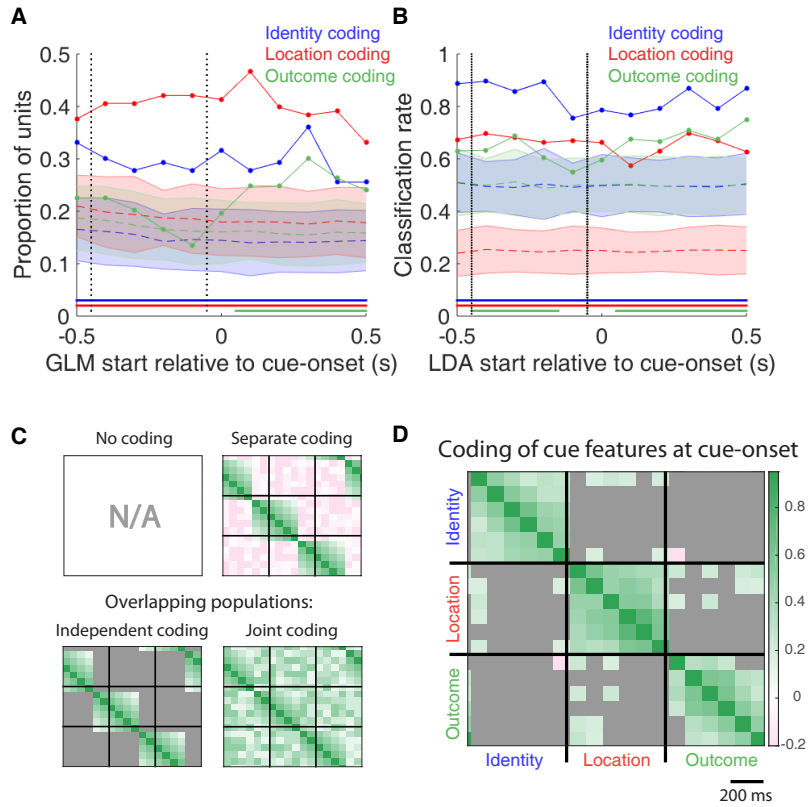


Figure 5: Summary of influence of various task parameters on cue-modulated NAc units after cue-onset. **A:** Sliding window GLM (bin size: 500 ms; step size: 100 ms) demonstrating the proportion of cue-modulated units where cue identity (blue solid line), location (red solid line), and outcome (green solid line) significantly contributed to the model at various time epochs relative to cue-onset. Dashed colored lines indicate the average of shuffling the firing rate order that went into the GLM 100 times. Error bars indicate 1.96 standard deviations from the shuffled mean. Solid lines at the bottom indicate when the proportion of units observed was greater than the shuffled samples (z-score ≥ 1.96). Points in between the two vertical dashed lines indicate bins where both pre- and post-cue-onset time periods were used in the GLM. **B:** Sliding window LDA (bin size: 500 ms; step size: 100 ms) demonstrating the classification rate for cue identity (blue solid line), location (red solid line), and outcome (green solid line) using a pseudoensemble of the 133 cue-modulated units. Dashed colored lines indicate the average of shuffling the firing rate order that went into the cross-validated LDA 100 times. Solid lines at the bottom indicate when the classifier performance greater than the shuffled samples (z-score ≥ 1.96). Points in between the two vertical dashed lines indicate bins where both pre- and post-cue-onset time periods were used in the classifier. **C-D:** Correlation matrices testing the presence and overlap of cue feature coding at cue-onset. **C:** Schematic outlining the different possible alternatives for coding across cue features at cue-onset, by correlating the recoded beta coefficients from the GLMs (see text for analysis details). Top left: coding is not present, therefore no comparison is possible. Top right: cue features are coded by separate populations of units. Displayed is a correlation matrix with each block representing correlations across the post- cue-onset time bins from the sliding window GLM for two various cue features, with green representing positive correlations ($r > 0$), pink representing negative correlations ($r < 0$), and grey representing no significant correlation ($r \sim 0$). X- and y-axis are the same, therefore the diagonal represents a correlation of an array against itself. Here the pink in the off-diagonal elements suggests that coding of cue features occur separately from one another. Bottom left: Coding of cue features occurs in overlapping but independent populations of units, shown here by the abundance of grey in the off-diagonal elements. Bottom right: Joint coding of cue features in an overlapping population, shown here by the green in the off-diagonal elements. **D:** Correlation matrix showing the correlation among identity, location, and outcome coding at cue-onset. Overabundance of grey, and relative lack of green in the off-diagonal elements suggests that coding of cue features occur independently of one another at cue-onset. Scale bar indicates relative bin size of the sliding window.

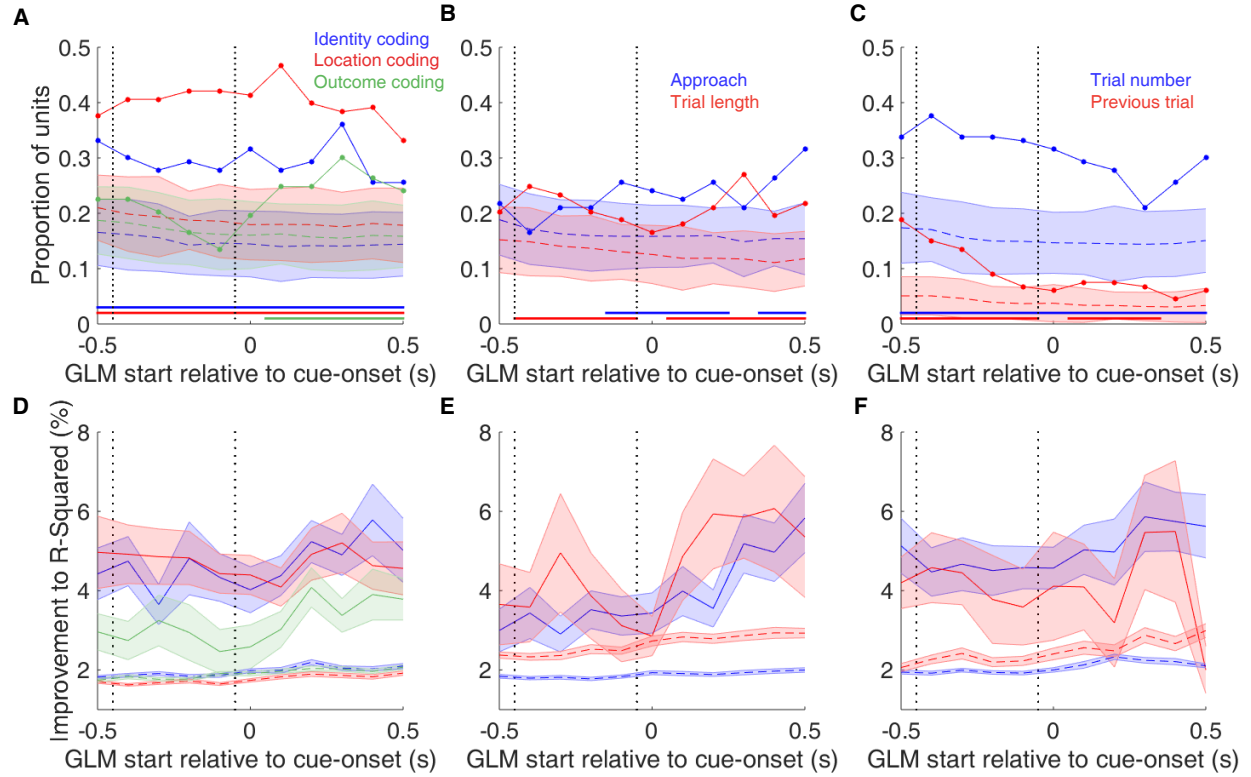


Figure supplement 1: Summary of influence of various task parameters on cue-modulated NAc units after cue-onset. **A-C:** Sliding window GLM illustrating the proportion of cue-modulated units influenced by various predictors around time of cue-onset. **A:** Sliding window GLM (bin size: 500 ms; step size: 100 ms) demonstrating the proportion of cue-modulated units where cue identity (blue solid line), location (red solid line), and outcome (green solid line) significantly contributed to the model at various time epochs relative to cue-onset. Dashed colored lines indicate the average of shuffling the firing rate order that went into the GLM 100 times. Error bars indicate 1.96 standard deviations from the shuffled mean. Solid lines at the bottom indicate when the proportion of units observed was greater than the shuffled samples (z -score > 1.96). Points in between the two vertical dashed lines indicate bins where both pre- and post-cue-onset time periods were used in the GLM. **B:** Same as A, but for approach behavior and trial length. **C:** Same as A, but for trial number and previous trial. **D-F:** Average improvement to model fit. **D:** Average percent improvement to R-squared for units where cue identity, location, or outcome were significant contributors to the final model for time epochs surrounding cue-onset. Shaded area around mean represents the standard error of the mean. **E:** Same as D, but for approach behavior and trial length. **F:** Same D, but for trial number and previous trial.

140 To assess what information may be encoded at the population level, we trained a classifier on a pseudoensemble
 141 of the 133 cue-modulated units (Figure ??). Specifically, we used the firing rate across units for each trial
 142 as an observation, and different cue features as trial labels (cue identity, outcome, and location). A linear dis-
 143 criminant analysis (LDA) classifier with 10-fold cross-validation could correctly predict a trial above chance
 144 levels for all cue features for most time epochs (z-score > 1.96 when comparing classification accuracy of
 145 data versus shuffling the firing rates). Notably, the ability to predict whether a trial was reward-available or
 146 reward-unavailable (cue outcome) was low pre-cue and increased as a trial progressed (Figure ??A).

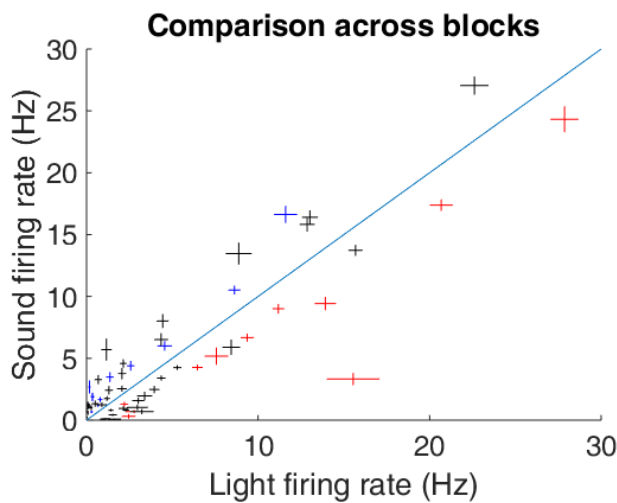


Figure supplement 2: Scatter plot depicting comparison of firing rates for cue-modulated units across light and sound blocks. Crosses are centered on the mean firing rate, range represents the SEM. Colored crosses represents units that had cue identity as a significant predictor of firing rate variance (blue are sound block preferring, red are light block preferring), whereas black crosses represent units where cue identity was not a significant predictor of firing rate variance. Diagonal dashed lines indicates point of equal firing across blocks.

147 **NAc units dynamically segment the task:**

148 Next, we sought to determine how coding of cue features evolved over time. Two main possibilities can be
149 distinguished (Figure 1, bottom), a unit coding for a feature such as cue outcome could remain persistently
150 active, or a progression of distinct units could activate in sequence. To visualize the distribution of responses
151 throughout our task space and test if this distribution is modulated by cue features, we z-scored the firing
152 rate of each unit and plotted the normalized firing rates of all units aligned to cue-onset and sorted them
153 according to the time of peak firing rate (Figure 6). We did this separately for both the light and sound
154 blocks, and found a nearly uniform distribution of firing fields in task space that was not limited to alignment
155 to the cue (Figure 6A). Furthermore, to determine if this population level activity was similar across blocks,
156 we also organized firing during the sound blocks according to the ordering derived from the light blocks.
157 This revealed that while there was some preservation of order, the overall firing was qualitatively different
158 across the two blocks, implying that population activity distinguishes between light and sound blocks. To
159 control for the possibility that any comparison of trials would produce this effect, we did a within block
160 comparison, comparing half of the trials in the light block against the other half. This comparison looked
161 similar to our test comparison of sound block trials ordered by light block trials. Additionally, given that the
162 majority of our units showed an inhibitory response to the cue, we also plotted the firing rates according to
163 the lowest time in firing, and again found some maintenance of order, but largely different ordering across
164 the two blocks, and the within block comparison (Figure 6D). To further test this, we divided each block into
165 two halves and looked at the correlation of the average smoothed firing rates across various combinations
166 of these halves across our cue-aligned centered epoch. A linear mixed effects model revealed that within
167 block correlations (e.g. one half of light trials vs other half of light trials) were higher and more similar
168 than across block correlations (e.g. half of light trials vs half of sound trials) suggesting that activity in
169 the NAc discriminates across various cue conditions (within block correlations = .383 (light), .379 (sound);
170 across block correlations = .343, .338, .337, .348; within block vs. within block comparison = $p = .934$;
171 within block vs. across block comparisons = $p < .001$). This process was repeated for cue location (Figure
172 6B,E; within block correlations = .369 (arm 1), .350 (arm 2); across block correlations = .290, .286, .285,

.291; within block vs. within block comparison = $p = .071$; within block vs. across block comparisons = $p < .001$) and cue outcome (Figure 6C,F; within block correlations = .429 (reward-available), .261 (reward-unavailable); across block correlations = .258, .253, .255, .249; within block vs. within block comparison = $p < .001$; within block vs. across block comparisons = $p < .001$), showing that NAc segmentation of the task is qualitatively different even during those parts of the task not immediately associated with a specific cue, action, or outcome, although the within condition comparison of reward-unavailable trials was less correlated than reward-available trials, and more similar to the across condition comparisons, potentially due to the greater behavioral variability for the reward-unavailable trials.

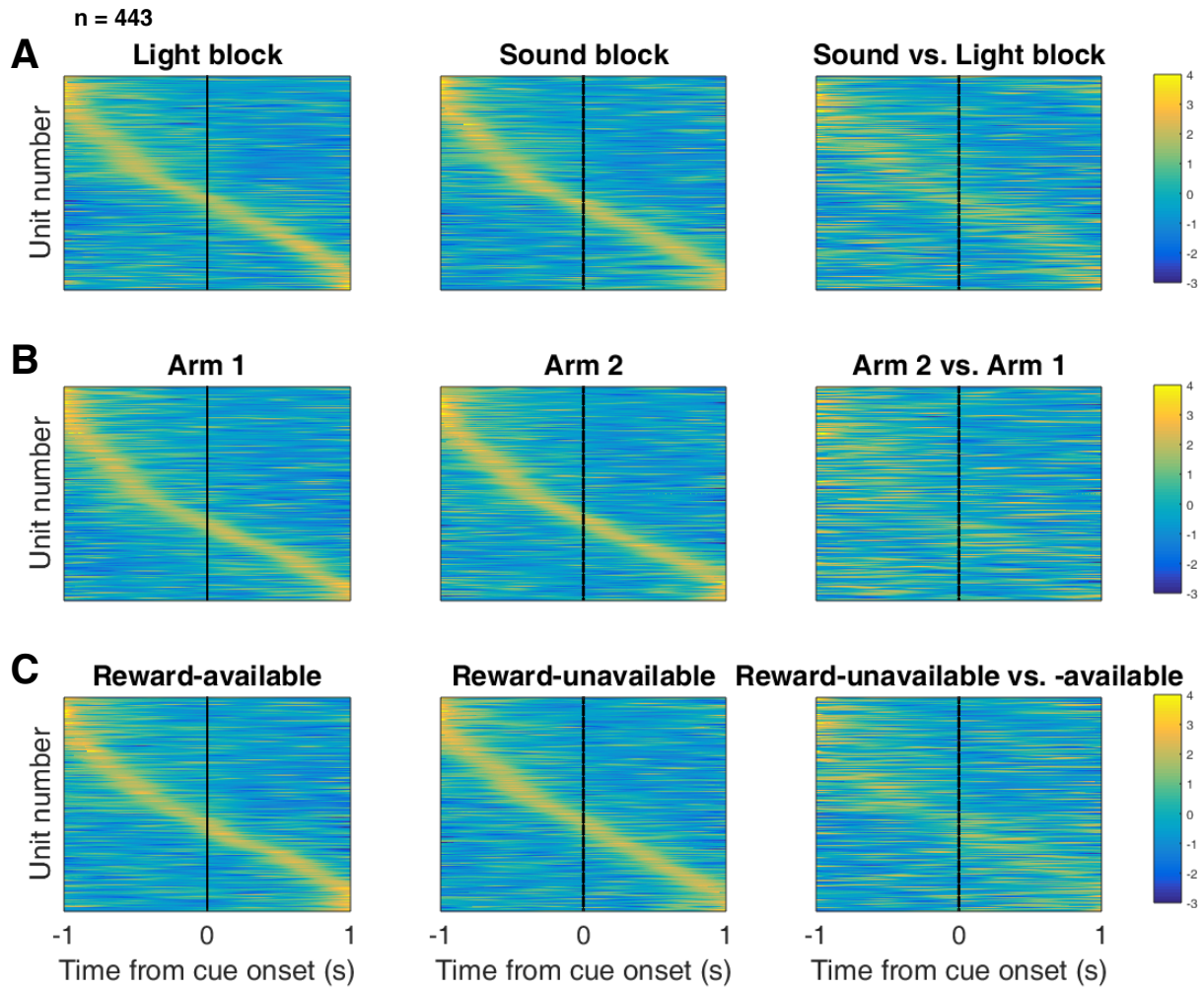


Figure 6: Distribution of NAc firing rates across time surrounding cue-onset. Each panel shows normalized (z-score) firing rates for all recorded NAc units (each row corresponds to one unit) as a function of time (time 0 indicates cue-onset), averaged across all trials for a specific cue type, indicated by text labels. **A-C:** Heat plots aligned to normalized peak firing rates. **A:** left: Heat plot showing smoothed normalized firing activity of all recorded NAc units ordered according to the time of their peak firing rate during the light block. Each row is a units average activity across time to the light block. Dashed line indicates cue-onset. Notice the yellow band across time, indicating all aspects of visualized task space were captured by the peak firing rates of various units. A, middle: Same units ordered according to the time of the peak firing rate during the sound block. Note that for both blocks, units tile time approximately uniformly with a clear diagonal of elevated firing rates. A, right: Unit firing rates taken from the sound block, ordered according to peak firing rate taken from the light block. Note that a weaker but still discernible diagonal persists, indicating partial similarity between firing rates in the two blocks. A similar pattern exists for within-block comparisons suggesting that reordering any two sets of trials produces this partial similarity, however correlations within blocks are more similar than correlations across blocks (see text). **B:** Same layout as in A, except that the panels now compare two different locations on the track instead of two cue modalities. As for the different cue modalities, NAc units clearly discriminate between locations, but also maintain some similarity across locations, as evident from the visible diagonal in the right panel. Two example locations were used for display purposes; other location pairs showed a similar pattern. **C:** Same layout as in A, except that panels now compare reward-available and reward-unavailable trials. Overall, NAc units "tiled" experience on the task, as opposed to being confined to specific task events only. Units from all sessions and animals were pooled for this analysis.

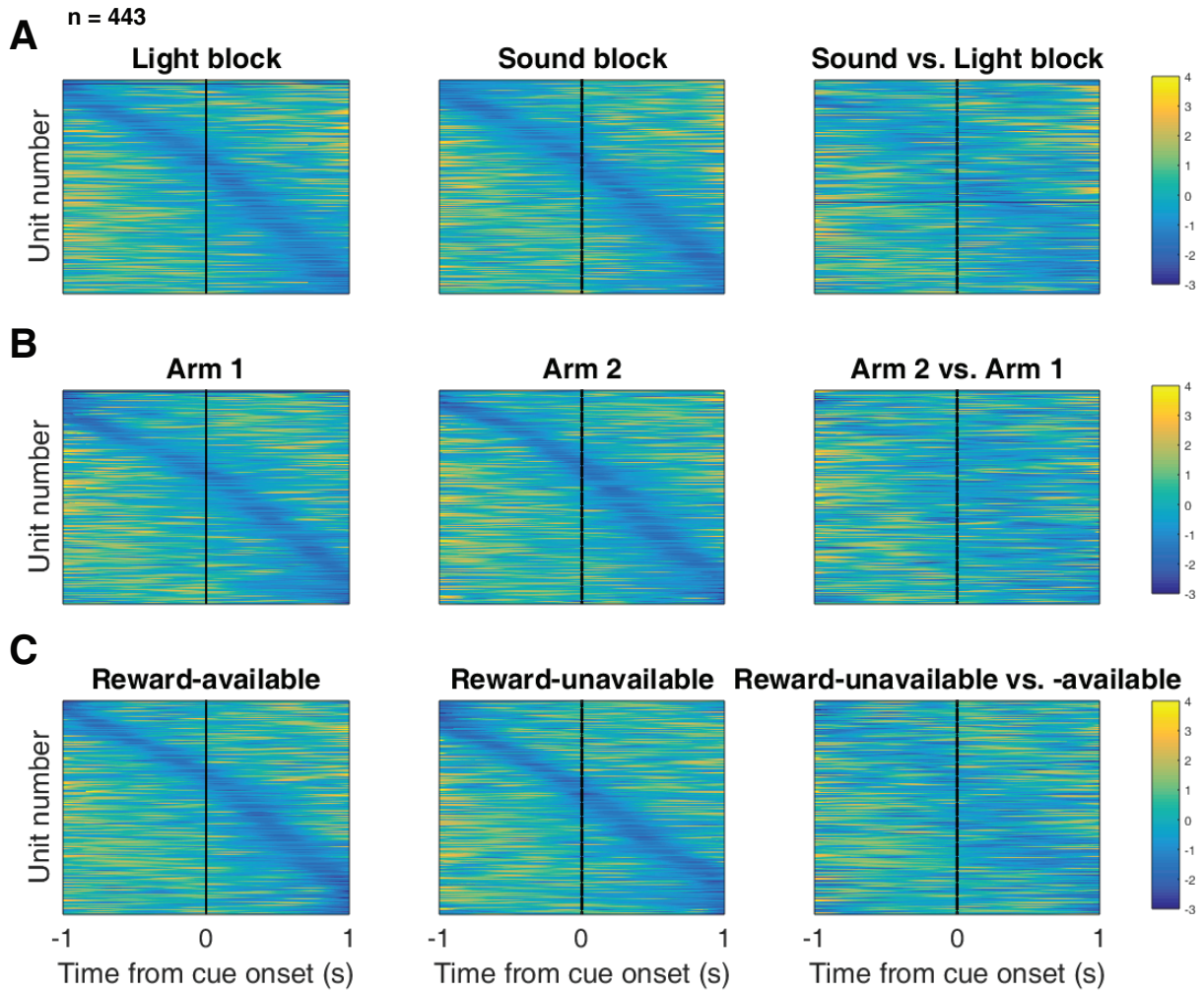


Figure supplement 1: Distribution of NAc firing rates across time surrounding cue-onset. Each panel shows normalized (z-score) firing rates for all recorded NAc units (each row corresponds to one unit) as a function of time (time 0 indicates cue-onset), averaged across all trials for a specific cue type, indicated by text labels. **A-C:** Heat plots aligned to normalized minimum firing rates. **A:** Responses during different stimulus blocks as in Figure 6A, but with units ordered according to the time of their minimum firing rate. **B:** Responses during trials on different arms as in Figure 6B, but with units ordered by their minimum firing rate. **C:** Responses during cues signalling different outcomes as in Figure 6C, but with units ordered by their minimum firing rate. Overall, NAc units "tiled" experience on the task, as opposed to being confined to specific task events only. Units from all sessions and animals were pooled for this analysis.

181 **NAc encoding of cue features persists until outcome:**

182 In order to be useful for credit assignment in reinforcement learning, a trace of the cue must be maintained
183 until the outcome, so that information about the outcome can be associated with the outcome-predictive cue.
184 To test whether representations of cue features persisted post-approach until the outcome was revealed, we
185 fit a GLM to the post-approach firing rates of cue-modulated units aligned to the time of nosepoke into the
186 reward receptacle. This analysis showed that a variety of units still discriminated firing according to various
187 cue features, but not other task parameters, showing that NAc activity discriminates various cue conditions
188 well into a trial (Table 1, Figures 7,??,??,??). Additionally, these units were a mix between most of the
189 units that encoded cue features at cue-onset ($r = .386, .781, .758$, across cue-onset and nosepoke for cue
190 identity, cue location, and cue outcome, respectively, all p values $< .001$), and those that did not previously
191 have a cue feature as a predictor (29, 48, and 30 out of 133 cue-modulated units encoded both time points
192 for cue identity, cue location, and cue outcome, respectively). Chi-square tests confirmed these results (cue
193 identity = $\chi^2 = 6.165$, $p = .013$; cue location = $\chi^2 = 21.670$, $p < .001$; cue outcome = $\chi^2 = 34.560$, $p < .001$).
194 Population level averages for units that increased to cue-onset showed a ramping up of activity that peaked
195 upon nosepoke, whereas units that decreased to cue-onset showed a gradual reduction of firing activity that
196 reached a minimum upon nosepoke (Figure ??). Additionally, a peak is seen for preferred cue outcome
197 in decreasing units at 1 second post cue-onset when reward was received, demonstrating an integration of
198 expected and received reward (Figure ??F).

199 Aligning normalized peak firing rates to nosepoke onset revealed a clustering of responses around outcome
200 receipt for all cue conditions where the rat would have received reward (Figure ??), in addition to the same
201 trend of higher within- vs across-block correlations for cue identity (Figure ??A,C; within block correlations
202 = .560 (light), .541 (sound); across block correlations = .487, .481, .483, .486; within block vs. within block
203 comparison = $p = .112$; within block vs. across block comparisons = $p < .001$) and cue location (Figure
204 ??B,E; within block correlations = .474 (arm 1), .461 (arm 2); across block correlations = .416, .402, .416,
205 .415; within block vs. within block comparison = $p = .810$; within block vs. across block comparisons = $p <$

.001), but not cue outcome (Figure ??C,F; within block correlations = .620 (reward-available), .401 (reward-unavailable); across block correlations = .418, .414, .390, .408; within block vs. within block comparison = p < .001; within block vs. across block comparisons = p < .001).

To determine whether coding of cue features persisted after the outcome was revealed, a GLM was fit to the firing rates of cue-modulated units at the time of outcome receipt, during which the cue was still present. Fitting a GLM revealed 10 units (8%) where cue outcome accounted for an average of 32% of firing rate variance (Table 1, data not shown). An absence of cue identity or cue location coding at this level of analysis was observed, but looking at the data more closely with a sliding window GLM revealed that cue identity, cue location, and cue outcome were encoded throughout time epochs surround cue-onset, nosepoke hold, and outcome receipt, suggesting that the NAc maintains a representation of these cue features once the rat receives behavioral feedback for its decision (Figure ??E-J).

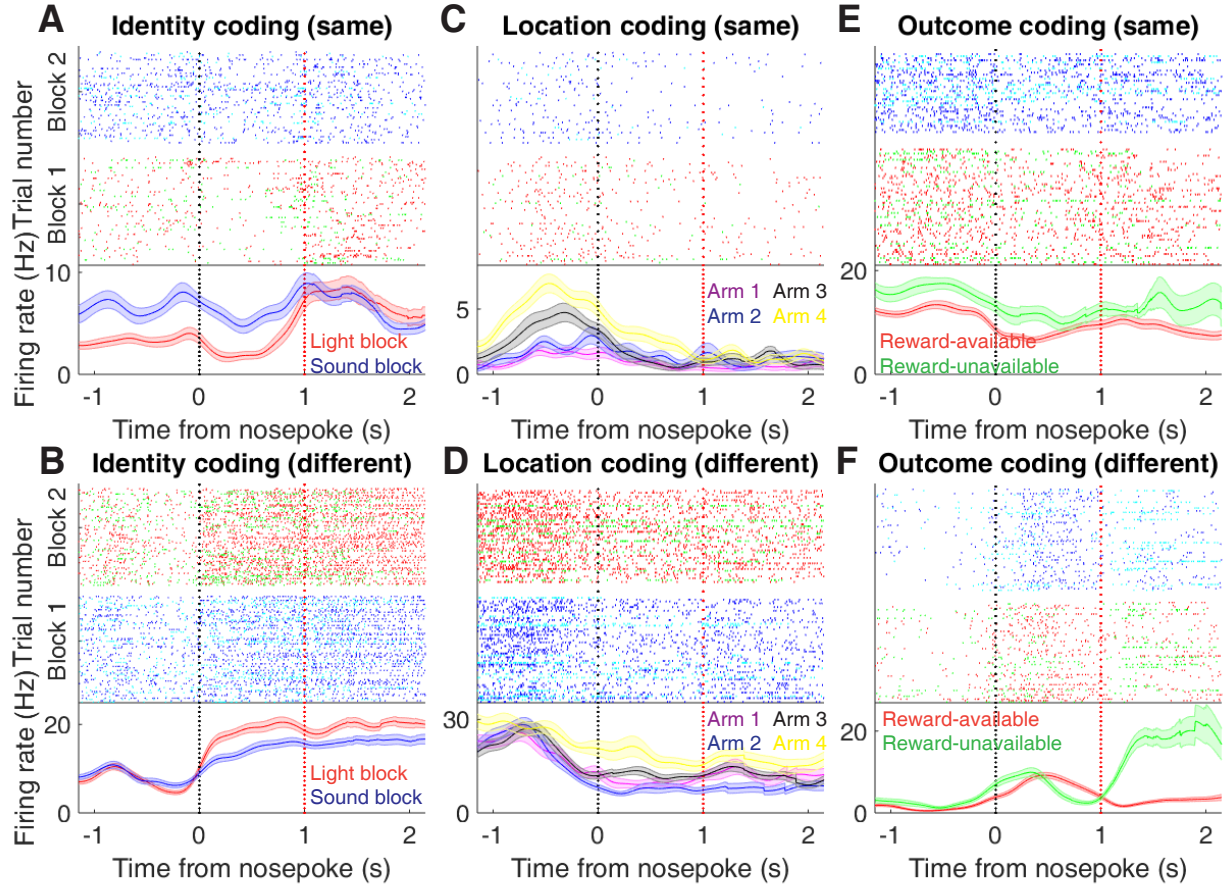


Figure 7: Examples of cue-modulated NAc units influenced by various task parameters at time of nosepoke. **A:** Example of a cue-modulated NAc unit that exhibited identity coding at both cue-onset and during nosepoke hold. Top: rasterplot showing the spiking activity across all trials aligned to nosepoke. Spikes across trials are color coded according to cue type (red: reward-available light; green: reward-unavailable light; navy blue: reward-available sound; light blue: reward-unavailable sound). White space halfway up the rasterplot indicates switching from one block to the next. Black dashed line indicates nosepoke. Red dashed line indicates receipt of outcome. Bottom: PETHs showing the average smoothed firing rate for the unit for trials during light (red) and sound (blue) blocks, aligned to nosepoke. Lightly shaded area indicates standard error of the mean. Note this unit showed a sustained increase in firing to sound cues during the trial. **B:** An example of a unit that was responsive to cue identity at time of nosepoke but not cue-onset. **C-D:** Cue-modulated units that exhibited location coding, at both cue-onset and nosepoke (C), and only nosepoke (D). Each color in the PETHs represents average firing response for a different cue location. **E-F:** Cue-modulated units that exhibited outcome coding, at both cue-onset and nosepoke (E), and only nosepoke (F), with the PETHs comparing reward-available (red) and reward-unavailable (green) trials.

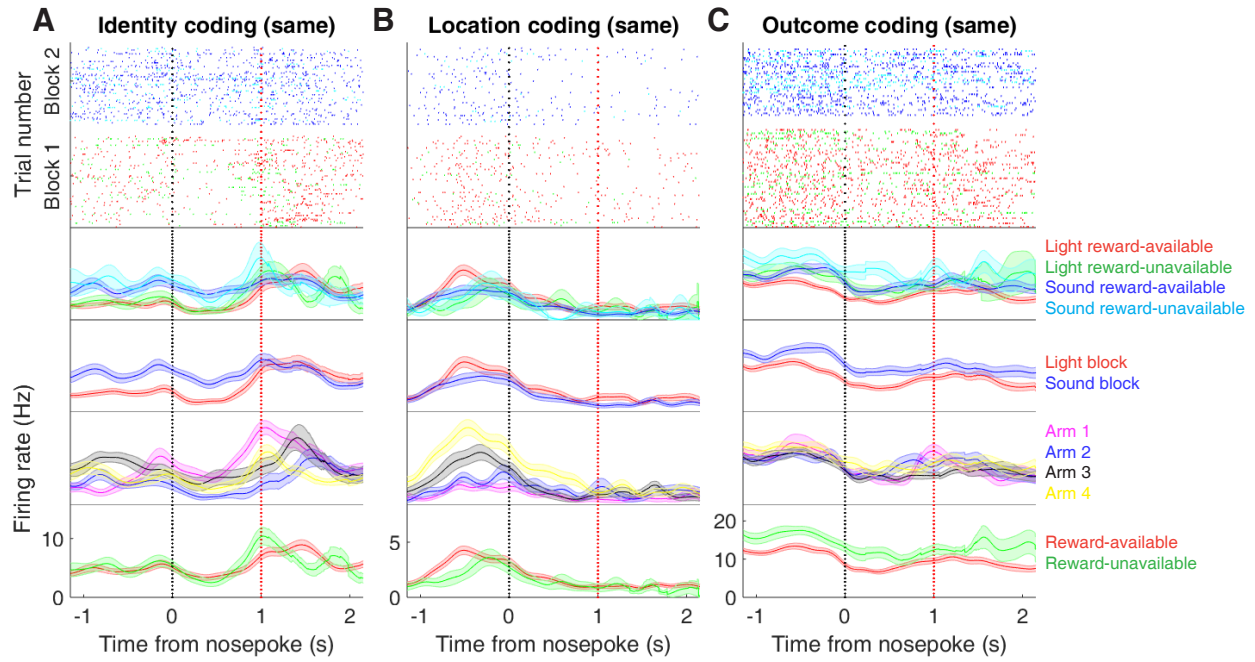


Figure supplement 1 Expanded examples of cue-modulated NAc units influenced by different task parameters at time of nosepoke for Figure 7A,C,E, showing firing rate breakdown by: cue type (top PETH), cue identity (top-middle PETH), cue location (bottom-middle PETH), and cue outcome (bottom PETH).

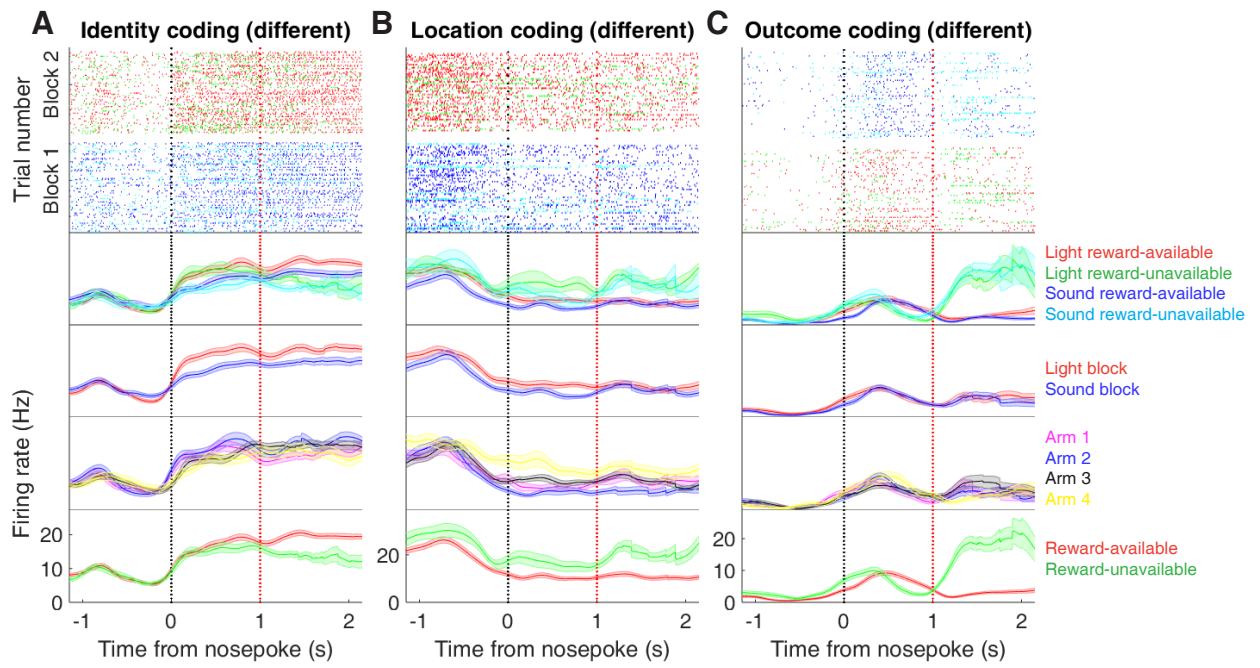


Figure supplement 2 Expanded examples of cue-modulated NAc units influenced by different task parameters at time of nosepoke for Figure 7B,D,F, showing firing rate breakdown by: cue type (top PETH), cue identity (top-middle PETH), cue location (bottom-middle PETH), and cue outcome (bottom PETH).

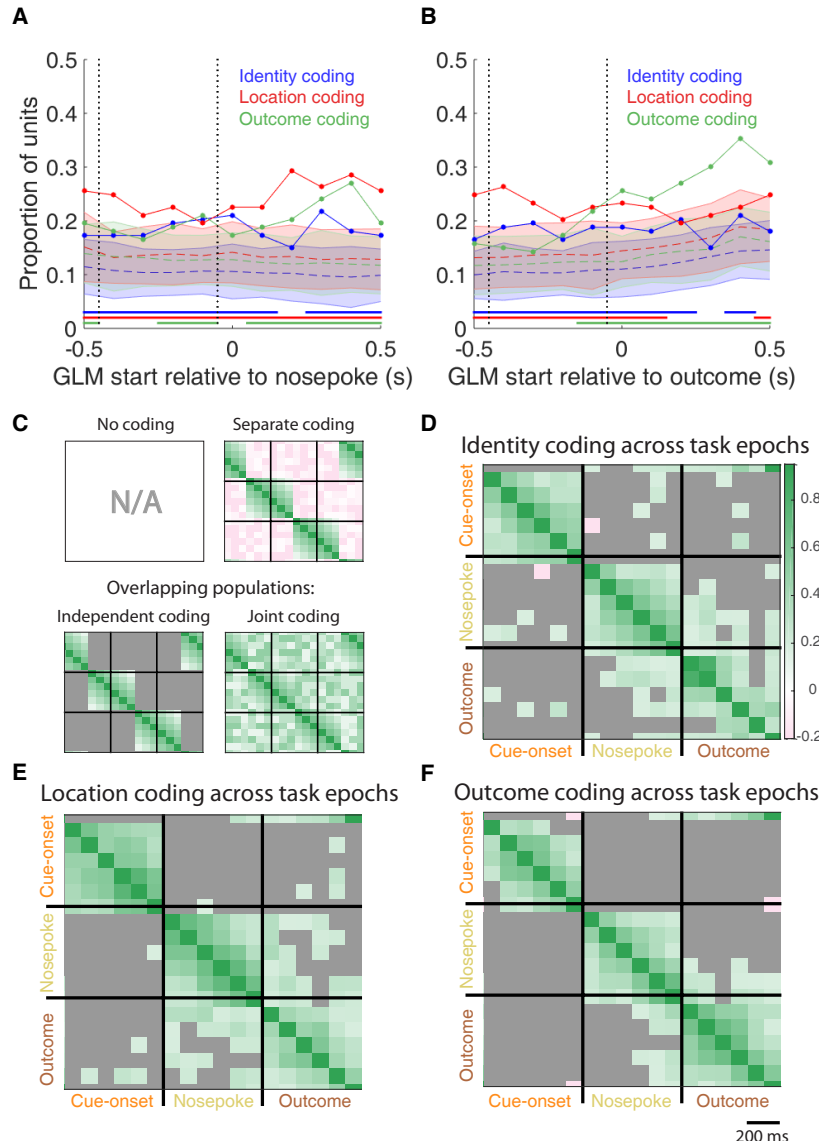


Figure 8: Summary of influence of various task parameters on cue-modulated NAc units during nosepoke and subsequent receipt of outcome. **A-B:** Sliding window GLM illustrating the proportion of cue-modulated units influenced by various predictors around time of nosepoke (A), and outcome (B). **A:** Sliding window GLM (bin size: 500 ms; step size: 100 ms) demonstrating the proportion of cue-modulated units where cue identity (blue solid line), location (red solid line), and outcome (green solid line) significantly contributed to the model at various time epochs relative to when the rat made a nosepoke. Dashed colored lines indicate the average of shuffling the firing rate order that went into the GLM 100 times. Error bars indicate 1.96 standard deviations from the shuffled mean. Solid lines at the bottom indicate when the proportion of units observed was greater than the shuffled samples (z -score > 1.96). Points in between the two vertical dashed lines indicate bins where both pre- and post-cue-onset time periods were used in the GLM. **B:** Same as A, but for time epochs relative to receipt of outcome after the rat got feedback about his approach. **C-F:** Correlation matrices testing the persistence of cue feature coding across points in time. **C:** Schematic outlining the different possible alternatives for coding of a cue feature across various points in a trial, by correlating the recoded beta coefficients from the GLMs (see text for analysis details). Top left: coding is not present, therefore no comparison is possible. Top right: a cue feature is coded by separate populations of units across time. Displayed is a correlation matrix with each block representing correlations across various event-centered time bins from the sliding window GLM for a single cue feature, with green representing positive correlations ($r > 0$), pink negative correlations ($r < 0$), and grey representing no significant correlation ($r \sim 0$). X- and y-axis are the same, therefore the diagonal represents a correlation of an array against itself. Here the pink in the off-diagonal elements suggests that coding of a cue feature is accomplished by separate populations of units across time. Bottom left: Coding of a cue feature across time occurs in overlapping but independent populations of units, shown here by the abundance of grey in the off-diagonal elements. Bottom right: Joint coding of a cue feature in an overlapping population across time, shown here by the

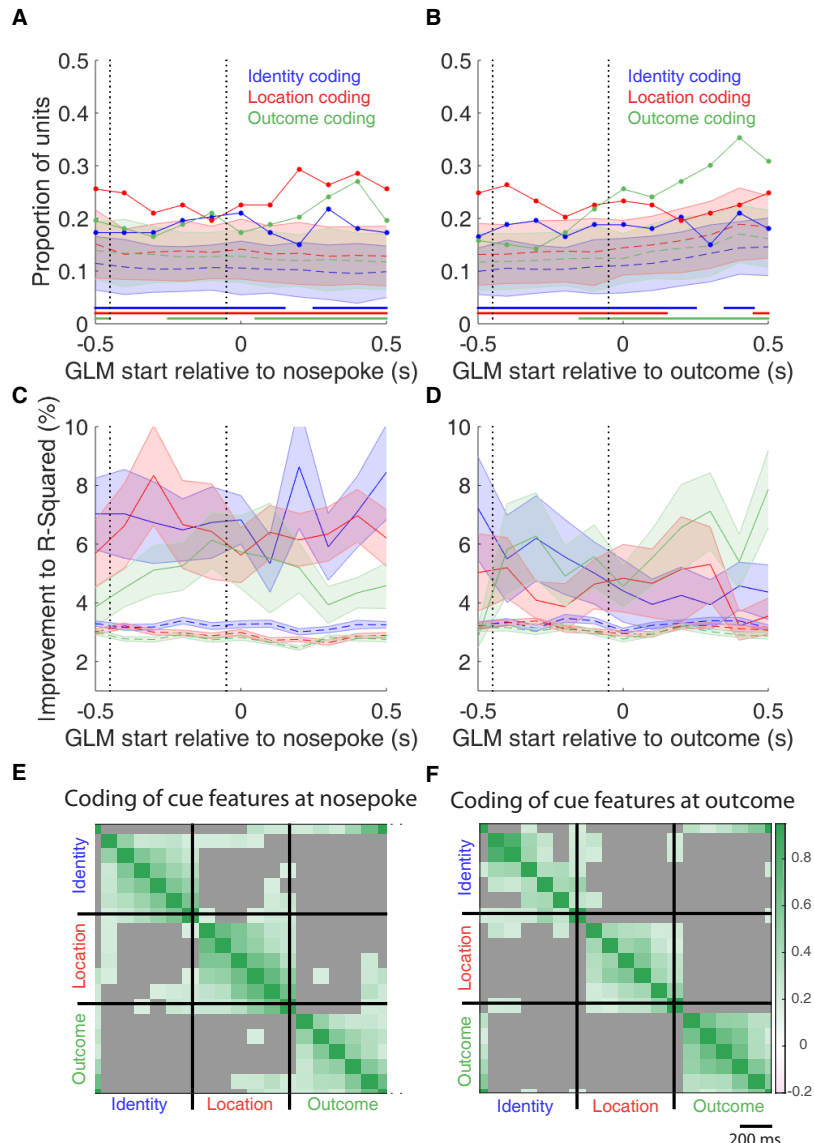


Figure supplement 1: Summary of influence of various task parameters on cue-modulated NAc units during nosepoke and subsequent receipt of outcome. **A-B:** Sliding window GLM illustrating the proportion of cue-modulated units influenced by various predictors around time of nosepoke (A), and outcome (B). **A:** Sliding window GLM (bin size: 500 ms; step size: 100 ms) demonstrating the proportion of cue-modulated units where cue identity (blue solid line), location (red solid line), and outcome (green solid line) significantly contributed to the model at various time epochs relative to when the rat made a nosepoke. Dashed colored lines indicate the average of shuffling the firing rate order that went into the GLM 100 times. Error bars indicate 1.96 standard deviations from the shuffled mean. Solid lines at the bottom indicate when the proportion of units observed was greater than the shuffled samples (z -score ≥ 1.96). Points in between the two vertical dashed lines indicate bins where both pre- and post-cue-onset time periods were used in the GLM. **B:** Same as A, but for time epochs relative to receipt of outcome after the rat got feedback about his approach. **C-D:** Average improvement to model fit. **C:** Average percent improvement to R-squared for units where cue identity (blue solid line), location (red solid line), or outcome (green solid line) were significant contributors to the final model for time epochs relative to nosepoke. Dashed colored lines indicate the average of shuffling the firing rate order that went into the GLM 100 times. Shaded area around mean represents the standard error of the mean. **D:** Same C, but for time epochs relative to receipt of outcome. **E-F:** Correlation matrices testing the presence and overlap of cue feature coding at nosepoke (E) and outcome (F). **E:** Correlation matrix showing the correlation among identity, location, and outcome coding at nosepoke. Each block represents correlations across various nosepoke-centered time bins from the sliding window GLM across cue features, with green representing positive correlations ($r > 0$), pink negative correlations ($r < 0$), and grey representing no significant correlation ($r \sim 0$). X- and y-axis are the same, therefore the diagonal represents a correlation of an array against itself. Scale bar indicates relative bin size of the sliding window. **F:** Same as E, but time bins following outcome.

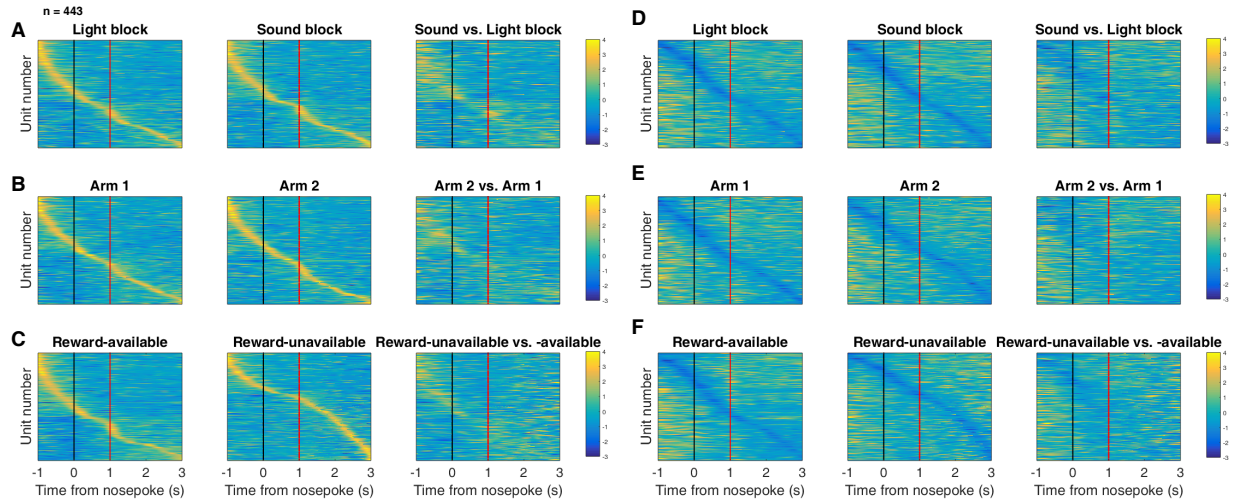


Figure supplement 2: Distribution of NAc firing rates across time surrounding nosepoke for approach trials. Each panel shows normalized (z-score) firing rates for all recorded NAc units (each row corresponds to one unit) as a function of time (time 0 indicates nosepoke), averaged across all approach trials for a specific cue type, indicated by text labels. **A-C:** Heat plots aligned to normalized peak firing rates. **A**, far left: Heat plot showing smoothed normalized firing activity of all recorded NAc units ordered according to the time of their peak firing rate during the light block. Each row is a units average activity across time to the light block. Black dashed line indicates nosepoke. Red dashed line indicates reward delivery occurring 1 s after nosepoke for reward-available trials. Notice the yellow band across time, indicating all aspects of visualized task space were captured by the peak firing rates of various units. **A**, middle: Same units ordered according to the time of the peak firing rate during the sound block. Note that for both blocks, units tile time approximately uniformly with a clear diagonal of elevated firing rates, and a clustering around outcome receipt. **A**, right: Unit firing rates taken from the sound block, ordered according to peak firing rate taken from the light block. Note that a weaker but still discernible diagonal persists, indicating partial similarity between firing rates in the two blocks. A similar pattern exists for within-block comparisons suggesting that reordering any two sets of trials produces this partial similarity, however correlations within blocks are more similar than correlations across blocks (see text). **B:** Same layout as in A, except that the panels now compare two different locations on the track instead of two cue modalities. As for the different cue modalities, NAc units clearly discriminate between locations, but also maintain some similarity across locations, as evident from the visible diagonal in the right panel. Two example locations were used for display purposes; other location pairs showed a similar pattern. **C:** Same layout as in A, except that panels now compare correct reward-available and incorrect reward-unavailable trials. The disproportionate tiling around outcome receipt for reward-available, but not reward-unavailable trials suggests encoding of reward receipt by NAc units. **D-F:** Heat plots aligned to normalized minimum firing rates. **D:** Responses during different stimulus blocks as in A, but with units ordered according to the time of their minimum firing rate. **E:** Responses during trials on different arms as in B, but with units ordered by their minimum firing rate. **F:** Responses during cues signalling different outcomes as in C, but with units ordered by their minimum firing rate. Overall, NAc units "tiled" experience on the task, as opposed to being confined to specific task events only. Units from all sessions and animals were pooled for this analysis.

217 **Discussion**

218 The main result of the present study is that NAc units encode not only the expected outcome of outcome-
219 predictive cues, but also the identity of such cues (Figure 1A). Importantly, this identity coding was main-
220 tained on approach trials both during a delay period where the rat held a nosepoke until the outcome was
221 received, and immediately after outcome receipt (Figure 1B). The population of units that coded for cue
222 identity was statistically independent from the population coding for expected outcome (i.e. overlap as ex-
223 pected from chance, Figure 1C). This information was also present at the population level, with a higher
224 than chance classification accuracy for predicting the right cue condition using a pseudoensemble. Units that
225 coded different cue features (identity, outcome, location) exhibited different temporal profiles as a whole,
226 although across all recorded units a tiling of task structure was observed such that all points within our an-
227 alyzed task space was accounted for by the ordered peak firing rates of all units. Furthermore, this tiling
228 differed between various conditions with a cue feature, such as light versus sound blocks. We discuss these
229 observations and their implications below.

230 **Cue identity:**

231 Our finding that NAc units can discriminate between different outcome-predictive stimuli with similar moti-
232 vational significance (i.e. encodes cue identity) expands upon an extensive rodent literature examining NAc
233 correlates of conditioned stimuli (Ambroggi, Ishikawa, Fields, & Nicola, 2008; Atallah et al., 2014; Bis-
234 sonette et al., 2013; Cooch et al., 2015; Day et al., 2006; Dejean et al., 2017; Goldstein et al., 2012; Ishikawa,
235 Ambroggi, Nicola, & Fields, 2008; Lansink et al., 2012; McGinty et al., 2013; Nicola, 2004; Roesch et al.,
236 2009; Roitman et al., 2005; Saddoris et al., 2011; Setlow et al., 2003; Sugam et al., 2014; West & Carelli,
237 2016; Yun, Wakabayashi, Fields, & Nicola, 2004). Perhaps the most comparable work in rodents comes
238 from a study that found distinct coding for an odor when it predicted separate but equally valued rewards
239 (Cooch et al., 2015). The present work is complementary to such *outcome identity* coding as it shows that
240 NAc units encode *cue identity*, in addition to the reward it predicts (Figure 1A). Similarly, Setlow et al.

241 (2003) paired distinct odor cues with appetitive or aversive outcomes, and found separate populations of
242 units that encoded each cue. Furthermore, during a reversal they found that the majority of units switched
243 their selectivity, arguing that the NAc units were tracking the motivational significance of these stimuli.
244 Once again, our study was different in asking how distinct cues encoding the same anticipated outcome are
245 encoded. Such cue identity encoding suggests that even when the motivational significance of these stimuli
246 is identical, NAc dissociates their representations at the level of the single-units. A possible interpretation
247 of this coding of cue features alongside expected outcome is that these representations are used to associate
248 reward with relevant features of the environment, so-called credit assignment in the reinforcement learning
249 literature (Sutton & Barto, 1998). A burgeoning body of human and non-human primate work has started to
250 elucidated neural correlates of credit assignment in the PFC, particularly in the lateral orbitofrontal cortex
251 (Akaishi, Kolling, Brown, & Rushworth, 2016; Asaad, Lauro, Perge, & Eskandar, 2017; Chau et al., 2015;
252 Noonan, Chau, Rushworth, & Fellows, 2017). Given the importance of cortical inputs in NAc associative
253 representations, it is possible that information related to credit assignment is relayed from the cortex to NAc
254 (Coch et al., 2015; Ishikawa et al., 2008).

255 Viewed within the neuroeconomic framework of decision making, functional magnetic resonance imaging
256 (fMRI) studies have found support for NAc representations of *offer value*, a domain-general common cur-
257 rency signal that enables comparison of different attributes such as reward identity, effort, and temporal
258 proximity (Bartra et al., 2013; Levy & Glimcher, 2012; Peters & Büchel, 2009; Sescousse et al., 2015). Our
259 study adds to a growing body of electrophysiological research that suggests the view of the NAc as a value
260 center, while informative and capturing major aspects of NAc processing, neglects additional contributions
261 of NAc to learning and decision making such as the offer (cue) identity signal reported here.

262 A different possible function for cue identity coding is to support contextual modulation of the motivational
263 relevance of specific cues. A context can be understood as a particular mapping between specific cues and
264 their outcomes: for instance, in context 1 cue A but not cue B is rewarded, whereas in context 2 cue B
265 but not cue A is rewarded. Successfully implementing such contextual mappings requires representation of

266 the cue identities. Indeed, Sleezer et al. (2016) recorded NAc responses during the Wisconsin Card Sorting
267 Task, a common set-shifting task used in both the laboratory and clinic, and found units that preferred firing
268 to stimuli when a certain rule, or rule category was currently active. Further support for a modulation of
269 NAc responses by strategy comes from an fMRI study that examined BOLD levels during a set-shifting task
270 (FitzGerald et al., 2014). In this task, participants learned two sets of stimulus-outcome contingencies, a
271 visual set and an auditory set. During testing they were presented with both simultaneously, and the stimulus
272 dimension that was relevant was periodically shifted between the two. Here, they found that bilateral NAc
273 activity reflected value representations for the currently relevant stimulus dimension, and not the irrelevant
274 stimulus. The current finding of independent coding of cue identity and expected outcome, suggests that the
275 fMRI finding is generated by the combined activity of several different functional cell types.

276 Our analyses were designed to eliminate several potential alternative interpretations to cue identity coding.
277 Because the different cues were separated into different blocks, units that discriminated between cue identi-
278 ties could instead be encoding time or other slowly-changing quantities. We excluded this possible confound
279 by excluding units that showed a drift in firing between the first and second half within a block. However, the
280 possibility remains that instead of or in addition to stimulus identity, these units encode a preferred context,
281 or even a macroscale representation of progress through the session. Indeed, encoding of the current strategy
282 could be an explanation for the sustained difference in population averaged firing across stimulus blocks
283 (Figure ??), as well as a potential explanation for the differentially tiling of task structure across blocks in
284 the current study (Figure 6).

285 A different potential confound is that between outcome and action value coding as the rat was only rewarded
286 for left turns. Our GLM analysis dealt with this by excluding firing rate variance accounted for by a predictor
287 that represented whether the animal approached (left turn) or skipped (right turn) the reward port at the
288 choice point, thus we were able to identify units that were modulated by the expected outcome of the cue
289 after removing variance for potential action value coding. Additionally, NAc signals have been shown to
290 be modulated by response vigor (McGinty et al., 2013); to detangle this from our results we included trial

291 length (i.e. latency to arrival at the reward site) as a predictor in our GLMs, and found units with cue feature
292 correlates independent of trial length.

293 An overall limitation of the current study is that rats were never presented with both sets of cues simul-
294 taneously, and were not required to switch strategies between multiple sets of cues (in behavioral pilots,
295 animals took several days of training to successfully switch strategies). Additionally, our recordings were
296 done during performance on the well-learned behavior, and not during the initial acquisition of the cue-
297 outcome relationships when an eligibility trace would be most useful. Thus, it is unknown to what extent
298 the cue identity encoding we observed is behaviorally relevant, although extrapolating data from other work
299 (Sleeker et al., 2016) suggests that cue identity coding would be modulated by relevance. NAc core lesions
300 have been shown to impair shifting between different behavioral strategies (Floresco et al., 2006), and it is
301 possible that selectively silencing the units that prefer responding for a given modality or rule would impair
302 performance when the animal is required to use that information, or artificial enhancement of those units
303 would cause them to use the rule when it is the inappropriate strategy.

304 **Encoding of position:**

305 Our finding that cue-evoked activity was modulated by cue location is in alignment with several previous
306 reports (Lavoie & Mizumori, 1994; Mulder, Shibata, Trullier, & Wiener, 2005; Strait et al., 2016; Wiener et
307 al., 2003). The NAc receives inputs from the hippocampus, and the communication of place-reward informa-
308 tion across the two structures suggests that the NAc tracks locations associated with reward (Lansink et al.,
309 2008; Lansink, Goltstein, Lankelma, McNaughton, & Pennartz, 2009; Lansink et al., 2016; Pennartz, 2004;
310 Sjulson, Peyrache, Cumpelik, Cassataro, & Buzsáki, 2017; Tabuchi, Mulder, & Wiener, 2000; van der Meer
311 & Redish, 2011). However, it is notable that in our task, location is explicitly uninformative about reward,
312 yet coding of this uninformative variable persists. The tiling of task space is in alignment with previous
313 studies showing that NAc units can also signal progress through a sequence of cues and/or actions (Atallah
314 et al., 2014; Berke, Breck, & Eichenbaum, 2009; Khamassi, Mulder, Tabuchi, Douchamps, & Wiener, 2008;

315 Lansink et al., 2012; Mulder, Tabuchi, & Wiener, 2004; Shidara, Aigner, & Richmond, 1998), is similar to
316 observations in the basal forebrain (Tingley & Buzsáki, 2018), and may represent a temporally evolved state
317 value signal (Hamid et al., 2015; Pennartz, Ito, Verschure, Battaglia, & Robbins, 2011). Given that the cur-
318 rent task was pseudo-random, it is possible that the rats learned the structure of sequential cue presentation,
319 and the neural activity could reflect this. However, this is unlikely as including a previous trial variable in
320 the analysis did not explain a significant amount of firing rate variance in response to the cue for the vast
321 majority of units. In any case, NAc units on the present task continued to distinguish between different
322 locations, even though location, and progress through a sequence, were explicitly irrelevant in predicting re-
323 ward. We speculate that this persistent coding of location in NAc may represent a bias in credit assignment,
324 and associated tendency for rodents to associate motivationally relevant events with the locations where they
325 occur.

326 **Implications:**

327 Maladaptive decision making, as occurs in schizophrenia, addiction, Parkinson's, among others, can re-
328 sult from dysfunctional RPE and value signals (Frank, Seeberger, & O'Reilly, 2004; Gradin et al., 2011;
329 Maia & Frank, 2011). This view has been successful in explaining both positive and negative symptoms in
330 schizophrenia, and deficits in learning from feedback in Parkinson's (Frank et al., 2004; Gradin et al., 2011).
331 However, the effects of RPE and value updating are contingent upon encoding of preceding action and cue
332 features, the eligibility trace (Lee et al., 2012; Sutton & Barto, 1998). Value updates can only be performed
333 on these aspects of preceding experience that are encoded when the update occurs. Therefore, maladaptive
334 learning and decision making can result from not only aberrant RPEs but also from altered cue feature en-
335 coding. For instance, on this task the environmental stimulus that signaled the availability of reward was
336 conveyed by two distinct cues that were presented in four locations. While in our current study, the location
337 and identity of the cue did not require any adjustments in the animals behavior, we found coding of these
338 features alongside the expected outcome of the cue that could be the outcome of credit assignment compu-
339 tations computed upstream. Identifying neural coding related to an aspect of credit assignment is important

340 as inappropriate credit assignment could be a contributor to conditioned fear overgeneralization seen in dis-
341 orders with pathological anxiety such as generalized anxiety disorder, post traumatic stress disorder, and
342 obsessive-compulsive disorder (Kaczkurkin et al., 2017; Kaczkurkin & Lissek, 2013; Lissek et al., 2014),
343 and delusions observed in disorders such as schizophrenia, Alzheimer's and Parkinson's (Corlett, Taylor,
344 Wang, Fletcher, & Krystal, 2010; Kapur, 2003). Thus, our results provide a neural window into the process
345 of credit assignment, such that the extent and specific manner in which this process fails in syndromes such
346 as schizophrenia, obsessive-compulsive disorder, etc. can be experimentally accessed.

347 **Methods**

348 **Subjects:**

349 A sample size of 4 adult male Long-Evans rats (Charles River, Saint Constant, QC) from an apriori deter-
350 mined sample of 5 were used as subjects (1 rat was excluded from the data set due to poor cell yield). Rats
351 were individually housed with a 12/12-h light-dark cycle, and tested during the light cycle. Rats were food
352 deprived to 85-90% of their free feeding weight (weight at time of implantation was 440 - 470 g), and water
353 restricted 4-6 hours before testing. All experimental procedures were approved by the the University of Wa-
354 terloo Animal Care Committee (protocol# 11-06) and carried out in accordance with Canadian Council for
355 Animal Care (CCAC) guidelines.

356 **Overall timeline:**

357 Each rat was first handled for seven days during which they were exposed to the experiment room, the
358 sucrose solution used as a reinforcer, and the click of the sucrose dispenser valves. Rats were then trained
359 on the behavioral task (described in the next section) until they reached performance criterion. At this point

360 they underwent hyperdrive implantation targeted at the NAc. Rats were allowed to recover for a minimum
361 of five days before being retrained on the task, and recording began once performance returned to pre-
362 surgery levels. Upon completion of recording, animals were glosed, euthanized and recording sites were
363 histologically confirmed.

364 **Behavioral task and training:**

365 The behavioral apparatus was an elevated, square-shaped track (100 x 100 cm, track width 10 cm) containing
366 four possible reward locations at the end of track “arms” (Figure 2). Rats initiated a *trial* by triggering a
367 photobeam located 24 cm from the start of each arm. Upon trial initiation, one of two possible light cues (L1,
368 L2), or one of two possible sound cues (S1, S2), was presented that signaled the presence (*reward-available*
369 *trial*, L1+, S1+) or absence (*reward-unavailable trial*, L2-, S2-) of a 12% sucrose water reward (0.1 mL) at
370 the upcoming reward site. A trial was classified as an *approach trial* if the rat turned left at the decision point
371 and made a nosepoke at the reward receptacle (40 cm from the decision point), while trials were classified as
372 a *skip trial* if the rat instead turned right at the decision point and triggered the photobeam to initiate the next
373 trial. A trial is labeled *correct* if the rat approached (i.e. nosepoked) on reward-available trials, and skipped
374 (i.e. did not nosepoke) on reward-unavailable trials. On reward-available trials there was a 1 second delay
375 between a nosepoke and subsequent reward delivery. *Trial length* was determined by measuring the length
376 of time from cue-onset until nosepoke (for approach trials), or from cue-onset until the start of the following
377 trial (for skip trials). Trials could only be initiated through clockwise progression through the series of arms,
378 and each entry into the subsequent arm on the track counted as a trial. Cues were present until 1 second after
379 outcome receipt on approach trials, and until initiating the following trial on skip trials.

380 Each session consisted of both a *light block* and a *sound block* with 100 trials each. Within a block, one cue
381 signaled reward was available on that trial (L1+ or S1+), while the other signaled reward was not available
382 (L2- or S2-). Light block cues were a flashing white light, and a constant yellow light. Sound block cues
383 were a 2 kHz sine wave and a 8 kHz sine wave whose amplitude was modulated from 0 to maximum by

384 a 2 Hz sine wave. Outcome-cue associations were counterbalanced across rats, e.g. for some rats L1+ was
385 the flashing white light, and for others L1+ was the constant yellow light. The order of cue presentation
386 was pseudorandomized so that the same cue could not be presented more than twice in a row. Block order
387 within each day was also pseudorandomized, such that the rat could not begin a session with the same block
388 for more than two days in a row. Each session consisted of a 5 minute pre-session period on a pedestal (a
389 terracotta planter filled with towels), followed by the first block, then the second block, then a 5 minute post-
390 session period on the pedestal. For approximately the first week of training, rats were restricted to running
391 in the clockwise direction by presenting a physical barrier to running counterclockwise. Cues signaling the
392 availability and unavailability of reward, as described above, were present from the start of training. Rats
393 were trained for 200 trials per day (100 trials per block) until they discriminated between the reward-available
394 and reward-unavailable cues for both light and sound blocks for three consecutive days, according to a chi-
395 square test rejecting the null hypothesis of equal approaches for reward-available and reward-unavailable
396 trials, at which point they underwent electrode implant surgery.

397 **Surgery:**

398 Surgical procedures were as described previously (Malhotra, Cross, Zhang, & Van Der Meer, 2015). Briefly,
399 animals were administered analgesics and antibiotics, anesthetized with isoflurane, induced with 5% in med-
400 ical grade oxygen and maintained at 2% throughout the surgery (0.8 L/min). Rats were then chronically
401 implanted with a “hyperdrive” consisting of 16 independently drivable tetrodes, either all 16 targeted for the
402 right NAc (AP +1.4 mm and ML +1.6 mm relative to bregma; Paxinos & Watson 1998), or 12 in the right
403 NAc and 4 targeted at the mPFC (AP +3.0 mm and ML +0.6 mm, relative to bregma; only data from NAc
404 tetrodes was analyzed). Following surgery, all animals were given at least five days to recover while receiv-
405 ing post-operative care, and tetrodes were lowered to the target (DV -6.0 mm) before being reintroduced to
406 the behavioral task.

407 **Data acquisition and preprocessing:**

408 After recovery, rats were placed back on the task for recording. NAc signals were acquired at 20 kHz with
409 a RHA2132 v0810 preamplifier (Intan) and a KJE-1001/KJD-1000 data acquisition system (Amplipex).
410 Signals were referenced against a tetrode placed in the corpus callosum above the NAc. Candidate spikes
411 for sorting into putative single units were obtained by band-pass filtering the data between 600-9000 Hz,
412 thresholding and aligning the peaks (UltraMegaSort2k, Hill, Mehta, & Kleinfeld, 2011). Spike waveforms
413 were then clustered with KlustaKwik using energy and the first derivative of energy as features, and manually
414 sorted into units (MClust 3.5, A.D. Redish et al., <http://redishlab.neuroscience.umn.edu/MClust/MClust.html>).
415 Isolated units containing a minimum of 200 spikes within a session were included for subsequent analysis.
416 Units were classified as fast spiking interneurons (FSIs) by an absence of interspike intervals (ISIs) > 2 s,
417 while medium spiny neurons (MSNs) had a combination of ISIs > 2 s and phasic activity with shorter ISIs
418 (Atallah et al., 2014; Barnes, Kubota, Hu, Jin, & Graybiel, 2005).

419 **Data analysis:**

420 *Behavior.* To determine if rats distinguished behaviorally between the reward-available and reward-unavailable
421 cues (*cue outcome*), we generated linear mixed effects models to investigate the relationships between cue
422 type and our behavioral variables, with *cue outcome* (reward available or not) and *cue identity* (light or
423 sound) as fixed effects, and the addition of an intercept for rat identity as a random effect. For each cue,
424 the average proportion of trials approached and trial length for a session were used as response variables.
425 Contribution of cue outcome to behavior was determined by comparing the full model to a model with cue
426 outcome removed for each behavioral variable.

427 *Neural data.* Given that some of our analyses compare firing rates across time, particularly comparisons
428 across blocks, we sought to exclude units with unstable firing rates that would generate spurious results
429 reflecting a drift in firing rate over time unrelated to our task. To do this we ran a Mann-Whitney U test
430 comparing the cue-evoked firing rates for the first and second half of trials within a block, and excluded 99
431 of 443 units from analysis that showed a significant change for either block, leaving 344 units for further

432 analyses by our GLM. To investigate the contribution of different cue features (*cue identity*, *cue location*
433 and *cue outcome*) on the firing rates of NAc single units, we first determined whether firing rates for a unit
434 were modulated by the onset of a cue by collapsing across all cues and comparing the firing rates for the 1
435 s preceding cue-onset with the 1 s following cue-onset. Single units were considered to be *cue-modulated* if
436 a Wilcoxon signed-rank test comparing pre- and post-cue firing was significant at $p < .01$. Cue-modulated
437 units were then classified as either increasing or decreasing if the post-cue activity was higher or lower than
438 the pre-cue activity, respectively.

439 To determine the relative contribution of different task parameters to firing rate variance (as in Figures 4-5),
440 a forward selection stepwise GLM using a Poisson distribution for the response variable was fit to each cue-
441 modulated unit, using data from every trial in a session. Cue identity (light block, sound block), cue location
442 (arm 1, arm 2, arm 3, arm 4), cue outcome (reward-available, reward-unavailable), behavior (approach,
443 skip), trial length, trial number, and trial history (reward availability on the previous 2 trials) were used as
444 predictors, and the 1 s post-cue firing rate as the response variable. Units were classified as being modulated
445 by a given task parameter if addition of the parameter significantly improved model fit using deviance as the
446 criterion ($p < .01$). A comparison of the R-squared value between the final model and the final model minus
447 the predictor of interest was used to determine the amount of firing rate variance explained by the addition
448 of that predictor for a given unit. To determine the degree to which coding of cue identity, cue location,
449 and cue outcome overlapped within units we computed pearsons r on recoded beta coefficients from the
450 GLM for the cue features. Specifically, for all cue-modulated units, we coded a 1 if the cue feature was a
451 significant predictor in the final model, and 0 if it was not, and calculated pearsons r comparing an array of
452 the coded 0s and 1s for cue-modulated units for one cue feature with a similar array for another cue feature.
453 The NAc was determined as coding a pair of cue features in a) a separate populations of units if there was a
454 significant negative correlation ($r < 0$), b) an independently coded overlapping population of units if there
455 was no significant correlation ($r = 0$), and c) a jointly coded overlapping population of units if there was a
456 significant positive correlation ($r > 0$). To investigate more finely the temporal dynamics of the influence of
457 task parameters to unit activity, we then fit a sliding window GLM with the same task parameters using 500

458 ms bins and 100 ms steps, starting 500 ms before cue-onset, up to 500 ms after cue-onset, and measured the
459 proportion of units and average R-squared value for a given time bin where a particular predictor contributed
460 significantly to the final model. To control for the amount of units that would be affected by a predictor by
461 chance, we shuffled the trial order of firing rates for a particular unit within a time bin, and took the average
462 of this value over 100 shuffles. We then calculated how many z-scores the observed proportion was from the
463 mean of the shuffles samples, using a z-score of greater than 1.96 as a marker of signifiance.

464 To get a sense for the predictive power of these cue feature representations we trained a classifier using firing
465 rates from a pseudoensemble of our 133 cue-modulated units (Figure ??). We created a matrix of firing rates
466 for each time epoch surrounding cue-onset where each row was an observation representing the firing rate
467 for a trial, and each column was a variable representing the firing rate for a given unit. Trial labels, or classes,
468 were each condition for a cue feature (e.g. light and sound for cue identity) when trying to predict each cue
469 feature, and combinations of conditions across cue features when trying to make more specific predictions
470 (e.g. light reward-available, light reward-unavailable, sound reward-available, sound reward-unavailable),
471 making sure to align trial labels across units. We then ran LDA on these matrices, using 10-fold cross
472 validation to train the classifier on 90% of the trials and testing its predictions on the held out 10% of trials,
473 and repeated this approach to get the classification accuracy for 100 iterations. To test if the classification
474 accuracy was greater by chance, we shuffled the order of firing rates for each unit before we trained the
475 classifier. We repeated this for 100 shuffled matrices for each time point, and calculated how many z-scores
476 the mean classification rate of the observed data was from the mean of the shuffled samples, using a z-score
477 of 1.96 as the cut off for a significant deviation from the permuted distribution.

478 To better visualize responses to cues and enable subsequent population level analyses (as in Figures 4, ??,
479 and 6), spike trains were convolved with a Gaussian kernel ($\sigma = 100$ ms), and peri-event time histograms
480 (PETHs) were generated by taking the average of the convolved spike trains across all trials for a given task
481 condition. For analysis of population-level responses for cue features (Figure ??), convolved spike trains
482 for all units where cue identity, cue location, or cue outcome explained a significant portion of firing rate

483 variance were z-scored. Within a given cue feature, normalized spike trains were then separated according
484 to the preferred and non-preferred cue condition (e.g. light vs. sound block), and averaged across units to
485 generate population-level averages. To account for separation that would result from any random selection
486 of units, unit identity was shuffled and the shuffled average for preferred and non-preferred cue conditions
487 was generated for 1000 shuffles.

488 To visualize NAc representations of task space within cue conditions, normalized spike trains for all units
489 were ordered by the location of their maximum or minimum firing rate for a specified cue condition (Figure
490 6). To compare representations of task space across cue conditions for a cue feature, the ordering of units
491 derived for one condition (e.g. light block) was then applied to the normalized spike trains for the other
492 condition (e.g. sound block). For control comparisons within cue conditions, half of the trials for a condition
493 were compared against the other half. To look at the correlation of firing rates of all units within and across
494 various cue conditions, trials for each cue condition for a unit were shuffled and divided into two averages,
495 and averages within and across cue conditions were correlated. A linear mixed effects model was run for
496 each cue condition to determine if correlations of firing rates within cue conditions were more similar than
497 correlations across cue conditions.

498 To identify the responsivity of units to different cue features at the time of a nosepoke into a reward re-
499 ceptacle, and subsequent reward delivery, the same cue-responsive units from the cue-onset analyses were
500 analyzed at the time of nosepoke and outcome receipt using identical analysis techniques for all approach
501 trials (Figures 7, ??, ??, and ??). To compare whether coding of a given cue feature was accomplished by
502 the same or distinct population of units across time epochs, we ran the recoded coefficient correlation that
503 was used to assess the degree of overlap among cue features within a time epoch.

504 All analyses were completed in MATLAB R2015a, the code is available on our public GitHub repository
505 (<http://github.com/vandermeelab/papers>), and the data can be accessed through DataLad.

506 **Histology:**

507 Upon completion of the experiment, recording channels were glosed by passing $10 \mu A$ current for 10 sec-
508 onds and waiting 5 days before euthanasia, except for rat R057 whose implant detached prematurely. Rats
509 were anesthetized with 5% isoflurane, then asphyxiated with carbon dioxide. Transcardial perfusions were
510 performed, and brains were fixed and removed. Brains were sliced in $50 \mu m$ coronal sections and stained
511 with thionin. Slices were visualized under light microscopy, tetrode placement was determined, and elec-
512 trodes with recording locations in the NAc were analyzed (Figure 9).

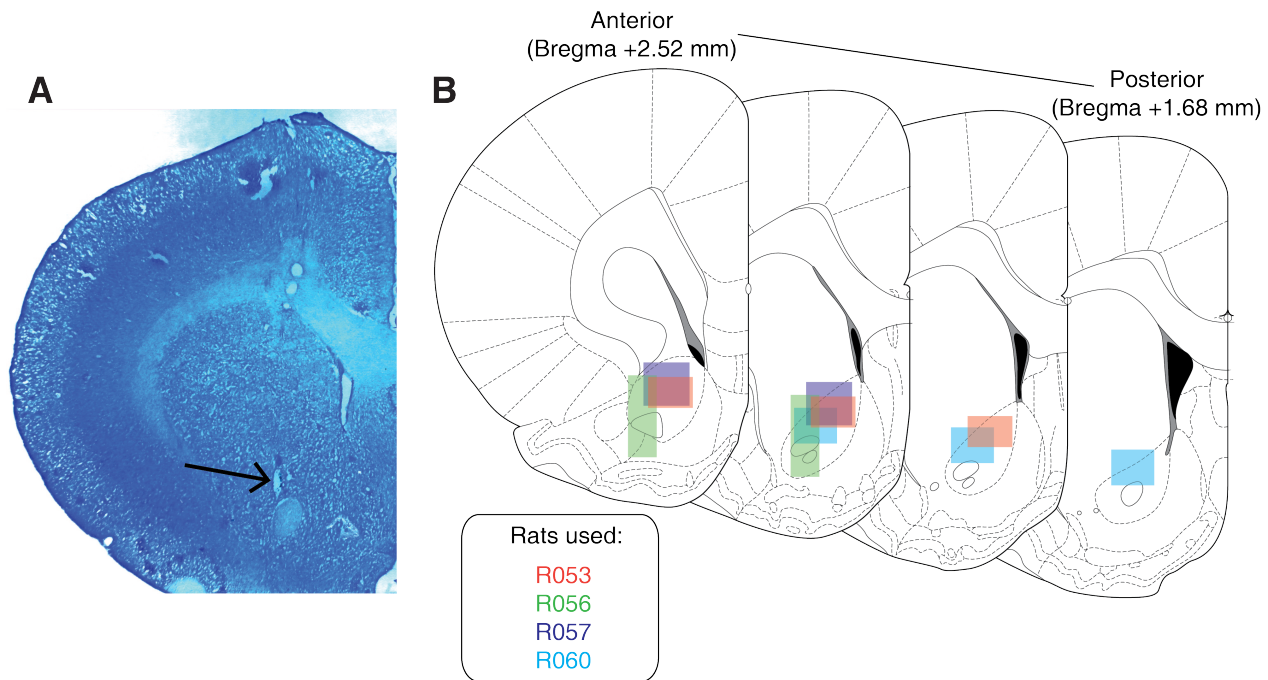


Figure 9: Histological verification of recording sites. Upon completion of experiments, brains were sectioned and tetrode placement was confirmed. **A:** Example section from R060 showing a recording site in the NAc core just dorsal to the anterior commissure (arrow). **B:** Schematic showing recording areas for all subjects.

513 **References**

- 514 Akaishi, R., Kolling, N., Brown, J. W., & Rushworth, M. (2016, jan). Neural Mechanisms of Credit Assignment in a Multicue
515 Environment. *Journal of Neuroscience*, 36(4), 1096–1112. doi: 10.1523/JNEUROSCI.3159-15.2016
- 516 Ambroggi, F., Ishikawa, A., Fields, H. L., & Nicola, S. M. (2008, aug). Basolateral Amygdala Neurons Facilitate Reward-Seeking
517 Behavior by Exciting Nucleus Accumbens Neurons. *Neuron*, 59(4), 648–661. doi: 10.1016/j.neuron.2008.07.004
- 518 Asaad, W. F., Lauro, P. M., Perge, J. A., & Eskandar, E. N. (2017, jul). Prefrontal Neurons Encode a Solution to the Credit-
519 Assignment Problem. *The Journal of Neuroscience*, 37(29), 6995–7007. doi: 10.1523/JNEUROSCI.3311-16.2017
- 520 Atallah, H. E., McCool, A. D., Howe, M. W., & Graybiel, A. M. (2014, jun). Neurons in the ventral striatum exhibit cell-type-
521 specific representations of outcome during learning. *Neuron*, 82(5), 1145–1156. doi: 10.1016/j.neuron.2014.04.021
- 522 Averbeck, B. B., & Costa, V. D. (2017, apr). Motivational neural circuits underlying reinforcement learning. *Nature Neuroscience*,
523 20(4), 505–512. doi: 10.1038/nrn.4506
- 524 Barnes, T. D., Kubota, Y., Hu, D., Jin, D. Z., & Graybiel, A. M. (2005, oct). Activity of striatal neurons reflects dynamic encoding
525 and recoding of procedural memories. *Nature*, 437(7062), 1158–1161. doi: 10.1038/nature04053
- 526 Bartra, O., McGuire, J. T., & Kable, J. W. (2013, aug). The valuation system: A coordinate-based meta-analysis
527 of BOLD fMRI experiments examining neural correlates of subjective value. *NeuroImage*, 76, 412–427. doi:
528 10.1016/J.NEUROIMAGE.2013.02.063
- 529 Berke, J. D., Breck, J. T., & Eichenbaum, H. (2009, mar). Striatal Versus Hippocampal Representations During Win-Stay Maze
530 Performance. *Journal of Neurophysiology*, 101(3), 1575–1587. doi: 10.1152/jn.91106.2008
- 531 Berridge, K. C. (2012, apr). From prediction error to incentive salience: Mesolimbic computation of reward motivation. *European
532 Journal of Neuroscience*, 35(7), 1124–1143. doi: 10.1111/j.1460-9568.2012.07990.x
- 533 Bissonette, G. B., Burton, A. C., Gentry, R. N., Goldstein, B. L., Hearn, T. N., Barnett, B. R., ... Roesch, M. R. (2013, may). Sepa-
534 rate Populations of Neurons in Ventral Striatum Encode Value and Motivation. *PLoS ONE*, 8(5), e64673. doi: 10.1371/jour-
535 nal.pone.0064673
- 536 Bouton, M. E. (1993, jul). Context, time, and memory retrieval in the interference paradigms of Pavlovian learning. *Psychological
537 Bulletin*, 114(1), 80–99. doi: 10.1371/journal.pone.0064673
- 538 Carelli, R. M. (2010). Drug Addiction: Behavioral Neurophysiology. In *Encyclopedia of neuroscience* (pp. 677–682). Elsevier.
539 doi: 10.1016/B978-008045046-9.01546-1
- 540 Chang, S. E., & Holland, P. C. (2013, nov). Effects of nucleus accumbens core and shell lesions on autoshaped lever-pressing.
541 *Behavioural Brain Research*, 256, 36–42. doi: 10.1016/j.bbr.2013.07.046
- 542 Chang, S. E., Wheeler, D. S., & Holland, P. C. (2012, may). Roles of nucleus accumbens and basolateral amygdala in autoshaped
543 lever pressing. *Neurobiology of Learning and Memory*, 97(4), 441–451. doi: 10.1016/j.nlm.2012.03.008

- 544 Chau, B. K. H., Sallet, J., Papageorgiou, G. K., Noonan, M. A. P., Bell, A. H., Walton, M. E., & Rushworth, M. F. S. (2015, sep).
545 Contrasting Roles for Orbitofrontal Cortex and Amygdala in Credit Assignment and Learning in Macaques. *Neuron*, 87(5),
546 1106–1118. doi: 10.1016/j.neuron.2015.08.018
- 547 Cheer, J. F., Aragona, B. J., Heien, M. L. A. V., Seipel, A. T., Carelli, R. M., & Wightman, R. M. (2007, apr). Coordinated
548 Accumbal Dopamine Release and Neural Activity Drive Goal-Directed Behavior. *Neuron*, 54(2), 237–244. doi:
549 10.1016/j.neuron.2007.03.021
- 550 Cohen, J. D., & Servan-Schreiber, D. (1992). Context, cortex, and dopamine: a connectionist approach to behavior and biology in
551 schizophrenia. *Psychological Review*, 99(1), 45.doi: 10.1016/j.neuron.2007.03.021
- 552 Cooch, N. K., Stalnaker, T. A., Wied, H. M., Bali-Chaudhary, S., McDannald, M. A., Liu, T. L., & Schoenbaum, G. (2015,
553 jun). Orbitofrontal lesions eliminate signalling of biological significance in cue-responsive ventral striatal neurons. *Nature
554 Communications*, 6, 7195. doi: 10.1038/ncomms8195
- 555 Corbit, L. H., & Balleine, B. W. (2011, aug). The General and Outcome-Specific Forms of Pavlovian-Instrumental Transfer Are
556 Differentially Mediated by the Nucleus Accumbens Core and Shell. *Journal of Neuroscience*, 31(33), 11786–11794. doi:
557 10.1523/JNEUROSCI.2711-11.2011
- 558 Corlett, P. R., Taylor, J. R., Wang, X.-J., Fletcher, P. C., & Krystal, J. H. (2010). Toward a neurobiology of delusions. *Progress in
559 Neurobiology*, 92, 345–369. doi: 10.1016/j.pneurobio.2010.06.007
- 560 Cromwell, H. C., & Schultz, W. (2003, may). Effects of Expectations for Different Reward Magnitudes on Neuronal Activity in
561 Primate Striatum. *Journal of Neurophysiology*, 89(5), 2823–2838. doi: 10.1152/jn.01014.2002
- 562 Day, J. J., Roitman, M. F., Wightman, R. M., & Carelli, R. M. (2007). Associative learning mediates dynamic shifts in dopamine
563 signaling in the nucleus accumbens. *Nature Neuroscience*, 10(8), 1020–1028. doi: 10.1038/nn1923
- 564 Day, J. J., Wheeler, R. A., Roitman, M. F., & Carelli, R. M. (2006, mar). Nucleus accumbens neurons encode Pavlovian ap-
565 proach behaviors: Evidence from an autoshaping paradigm. *European Journal of Neuroscience*, 23(5), 1341–1351. doi:
566 10.1111/j.1460-9568.2006.04654.x
- 567 Dejean, C., Sitko, M., Girardeau, P., Bennabi, A., Caillé, S., Cador, M., ... Le Moine, C. (2017, apr). Memories of Opiate
568 Withdrawal Emotional States Correlate with Specific Gamma Oscillations in the Nucleus Accumbens. *Neuropsychophar-
569 macology*, 42(5), 1157–1168. doi: 10.1038/npp.2016.272
- 570 du Hoffmann, J., & Nicola, S. M. (2014, oct). Dopamine Invigorates Reward Seeking by Promoting Cue-Evoked Excitation in the
571 Nucleus Accumbens. *Journal of Neuroscience*, 34(43), 14349–14364. doi: 10.1523/JNEUROSCI.3492-14.2014
- 572 Estes, W. K. (1943). Discriminative conditioning. I. A discriminative property of conditioned anticipation. *Journal of Experimental
573 Psychology*, 32(2), 150–155. doi: 10.1037/h0058316
- 574 Fitzgerald, T. H. B., Schwartenbeck, P., & Dolan, R. J. (2014). Reward-Related Activity in Ventral Striatum Is Action Contingent
575 and Modulated by Behavioral Relevance. *Journal of Neuroscience*, 34(4), 1271–1279. doi: 10.1523/JNEUROSCI.4389-
576 13.2014

- 577 Flagel, S. B., Clark, J. J., Robinson, T. E., Mayo, L., Czuj, A., Willuhn, I., ... Akil, H. (2011, jan). A selective role for dopamine
578 in stimulus-reward learning. *Nature*, 469(7328), 53–59. doi: 10.1038/nature09588
- 579 Floresco, S. B. (2015, jan). The Nucleus Accumbens: An Interface Between Cognition, Emotion, and Action. *Annual Review of
580 Psychology*, 66(1), 25–52. doi: 10.1146/annurev-psych-010213-115159
- 581 Floresco, S. B., Ghods-Sharifi, S., Vexelman, C., & Magyar, O. (2006, mar). Dissociable roles for the nucleus accumbens core and
582 shell in regulating set shifting. *Journal of Neuroscience*, 26(9), 2449–2457. doi: 10.1523/JNEUROSCI.4431-05.2006
- 583 Frank, M. J., Seeberger, L. C., & O'Reilly, R. C. (2004, dec). By carrot or by stick: Cognitive reinforcement learning in Parkinson-
584 ism. *Science*, 306(5703), 1940–1943. doi: 10.1126/science.1102941
- 585 Giertler, C., Bohn, I., & Hauber, W. (2004, feb). Transient inactivation of the rat nucleus accumbens does not impair guidance of
586 instrumental behaviour by stimuli predicting reward magnitude. *Behavioural Pharmacology*, 15(1), 55–63. doi: 10.1126/sci-
587 ence.1102941
- 588 Goldstein, B. L., Barnett, B. R., Vasquez, G., Tobia, S. C., Kashtelyan, V., Burton, A. C., ... Roesch, M. R. (2012, feb). Ventral
589 Striatum Encodes Past and Predicted Value Independent of Motor Contingencies. *Journal of Neuroscience*, 32(6), 2027–
590 2036. doi: 10.1523/JNEUROSCI.5349-11.2012
- 591 Goto, Y., & Grace, A. A. (2008, nov). Limbic and cortical information processing in the nucleus accumbens. *Trends in Neuro-
592 sciences*, 31(11), 552–558. doi: 10.1016/j.tins.2008.08.002
- 593 Gradin, V. B., Kumar, P., Waiter, G., Ahearn, T., Stickle, C., Milders, M., ... Steele, J. D. (2011, jun). Expected value and prediction
594 error abnormalities in depression and schizophrenia. *Brain*, 134(6), 1751–1764. doi: 10.1093/brain/awr059
- 595 Grant, D. A., & Berg, E. (1948). A behavioral analysis of degree of reinforcement and ease of shifting to new responses in a
596 Weigl-type card-sorting problem. *Journal of Experimental Psychology*, 38(4), 404–411. doi: 10.1037/h0059831
- 597 Hamid, A. A., Pettibone, J. R., Mabrouk, O. S., Hetrick, V. L., Schmidt, R., Vander Weele, C. M., ... Berke, J. D. (2015, jan).
598 Mesolimbic dopamine signals the value of work. *Nature Neuroscience*, 19(1), 117–126. doi: 10.1038/nn.4173
- 599 Hart, A. S., Rutledge, R. B., Glimcher, P. W., & Phillips, P. E. M. (2014, jan). Phasic Dopamine Release in the Rat Nucleus
600 Accumbens Symmetrically Encodes a Reward Prediction Error Term. *The Journal of Neuroscience*, 34(3), 698–704. doi:
601 10.1523/JNEUROSCI.2489-13.2014
- 602 Hassani, O. K., Cromwell, H. C., & Schultz, W. (2001, jun). Influence of Expectation of Different Rewards on Behavior-Related
603 Neuronal Activity in the Striatum. *Journal of Neurophysiology*, 85(6), 2477–2489. doi: 10.1152/jn.2001.85.6.2477
- 604 Hearst, E., & Jenkins, H. M. (1974). *Sign-tracking: the stimulus-reinforcer relation and directed action*. Psychonomic Society. doi:
605 10.1152/jn.2001.85.6.2477
- 606 Hill, D. N., Mehta, S. B., & Kleinfeld, D. (2011, jun). Quality Metrics to Accompany Spike Sorting of Extracellular Signals.
607 *Journal of Neuroscience*, 31(24), 8699–8705. doi: 10.1523/JNEUROSCI.0971-11.2011
- 608 Holland, P. C. (1992, jan). Occasion setting in pavlovian conditioning. *Psychology of Learning and Motivation*, 28(C), 69–125.
609 doi: 10.1016/S0079-7421(08)60488-0

- 610 Hollerman, J. R., Tremblay, L., & Schultz, W. (1998, aug). Influence of Reward Expectation on Behavior-Related Neuronal Activity
611 in Primate Striatum. *Journal of Neurophysiology*, 80(2), 947–963. doi: 10.1152/jn.1998.80.2.947
- 612 Honey, R. C., Iordanova, M. D., & Good, M. (2014, feb). Associative structures in animal learning: Dissociating elemental and
613 configural processes. *Neurobiology of Learning and Memory*, 108, 96–103. doi: 10.1016/j.nlm.2013.06.002
- 614 Hyman, S. E., Malenka, R. C., & Nestler, E. J. (2006, jul). NEURAL MECHANISMS OF ADDICTION: The Role
615 of Reward-Related Learning and Memory. *Annual Review of Neuroscience*, 29(1), 565–598. doi: 10.1146/an-
616 nurev.neuro.29.051605.113009
- 617 Ikemoto, S. (2007, nov). Dopamine reward circuitry: Two projection systems from the ventral midbrain to the nucleus accumbens-
618 olfactory tubercle complex. *Brain Research Reviews*, 56(1), 27–78. doi: 10.1016/j.brainresrev.2007.05.004
- 619 Ishikawa, A., Ambroggi, F., Nicola, S. M., & Fields, H. L. (2008, may). Dorsomedial Prefrontal Cortex Contribution to Behav-
620 ioral and Nucleus Accumbens Neuronal Responses to Incentive Cues. *Journal of Neuroscience*, 28(19), 5088–5098. doi:
621 10.1523/JNEUROSCI.0253-08.2008
- 622 Joel, D., Niv, Y., & Ruppin, E. (2002, jun). Actor-critic models of the basal ganglia: new anatomical and computational perspectives.
623 *Neural Networks*, 15(4-6), 535–547. doi: 10.1016/S0893-6080(02)00047-3
- 624 Kaczkurkin, A. N., Burton, P. C., Chazin, S. M., Manbeck, A. B., Espensen-Sturges, T., Cooper, S. E., ... Lissek, S. (2017, feb).
625 Neural substrates of overgeneralized conditioned fear in PTSD. *American Journal of Psychiatry*, 174(2), 125–134. doi:
626 10.1176/appi.ajp.2016.15121549
- 627 Kaczkurkin, A. N., & Lissek, S. (2013). Generalization of Conditioned Fear and Obsessive-Compulsive Traits. *Journal of Psychol-
628 ogy & Psychotherapy*, 7, 3. doi: 10.4172/2161-0487.S7-003
- 629 Kalivas, P. W., & Volkow, N. D. (2005, aug). The neural basis of addiction: A pathology of motivation and choice. *American
630 Journal of Psychiatry*, 162(8), 1403–1413. doi: 10.1176/appi.ajp.162.8.1403
- 631 Kapur, S. (2003, jan). Psychosis as a state of aberrant salience: A framework linking biology, phenomenology, and pharmacology
632 in schizophrenia. *American Journal of Psychiatry*, 160(1), 13–23. doi: 10.1176/appi.ajp.160.1.13
- 633 Khamassi, M., & Humphries, M. D. (2012). Integrating cortico-limbic-basal ganglia architectures for learning model-based and
634 model-free navigation strategies. *Frontiers in Behavioral Neuroscience*, 6, 79. doi: 10.3389/fnbeh.2012.00079
- 635 Khamassi, M., Mulder, A. B., Tabuchi, E., Douchamps, V., & Wiener, S. I. (2008, nov). Anticipatory reward signals in ventral striatal
636 neurons of behaving rats. *European Journal of Neuroscience*, 28(9), 1849–1866. doi: 10.1111/j.1460-9568.2008.06480.x
- 637 Lansink, C. S., Goltstein, P. M., Lankelma, J. V., Joosten, R. N. J. M. A., McNaughton, B. L., & Pennartz, C. M. A. (2008, jun).
638 Preferential Reactivation of Motivationally Relevant Information in the Ventral Striatum. *Journal of Neuroscience*, 28(25),
639 6372–6382. doi: 10.1523/JNEUROSCI.1054-08.2008
- 640 Lansink, C. S., Goltstein, P. M., Lankelma, J. V., McNaughton, B. L., & Pennartz, C. M. (2009, aug). Hippocampus leads ventral
641 striatum in replay of place-reward information. *PLoS Biology*, 7(8), e1000173. doi: 10.1371/journal.pbio.1000173
- 642 Lansink, C. S., Jackson, J. C., Lankelma, J. V., Ito, R., Robbins, T. W., Everitt, B. J., & Pennartz, C. M. A. (2012, sep). Reward

- 643 Cues in Space: Commonalities and Differences in Neural Coding by Hippocampal and Ventral Striatal Ensembles. *Journal*
644 *of Neuroscience*, 32(36), 12444–12459. doi: 10.1523/JNEUROSCI.0593-12.2012
- 645 Lansink, C. S., Meijer, G. T., Lankelma, J. V., Vinck, M. A., Jackson, J. C., & Pennartz, C. M. A. (2016, oct). Reward Ex-
646 pectancy Strengthens CA1 Theta and Beta Band Synchronization and Hippocampal-Ventral Striatal Coupling. *Journal of*
647 *Neuroscience*, 36(41), 10598–10610. doi: 10.1523/JNEUROSCI.0682-16.2016
- 648 Lavoie, A. M., & Mizumori, S. J. (1994, feb). Spatial, movement- and reward-sensitive discharge by medial ventral striatum neurons
649 of rats. *Brain Research*, 638(1-2), 157–168. doi: 10.1016/0006-8993(94)90645-9
- 650 Lee, D., Seo, H., & Jung, M. W. (2012). Neural Basis of Reinforcement Learning and Decision Making. *Annual Review of*
651 *Neuroscience*, 35(1), 287–308. doi: 10.1146/annurev-neuro-062111-150512
- 652 Levy, D. J., & Glimcher, P. W. (2012). The root of all value: a neural common currency for choice. *Current Opinion in Neurobiology*,
653 22, 1027–1038. doi: 10.1016/j.conb.2012.06.001
- 654 Lissek, S., Kaczkurkin, A. N., Rabin, S., Geraci, M., Pine, D. S., & Grillon, C. (2014, jun). Generalized anxiety disor-
655 der is associated with overgeneralization of classically conditioned fear. *Biological Psychiatry*, 75(11), 909–915. doi:
656 10.1016/j.biopsych.2013.07.025
- 657 Maia, T. V. (2009, dec). Reinforcement learning, conditioning, and the brain: Successes and challenges. *Cognitive, Affective and*
658 *Behavioral Neuroscience*, 9(4), 343–364. doi: 10.3758/CABN.9.4.343
- 659 Maia, T. V., & Frank, M. J. (2011). From reinforcement learning models to psychiatric and neurological disorders. *Nature*
660 *Neuroscience*, 14(2), 154–162. doi: 10.1038/nn.2723
- 661 Malhotra, S., Cross, R. W., Zhang, A., & Van Der Meer, M. A. A. (2015). Ventral striatal gamma oscillations are highly variable
662 from trial to trial, and are dominated by behavioural state, and only weakly influenced by outcome value. *European Journal*
663 *of Neuroscience*, 42(10), 2818–2832. doi: 10.1038/nn.2723
- 664 McDannald, M. A., Lucantonio, F., Burke, K. A., Niv, Y., & Schoenbaum, G. (2011, feb). Ventral Striatum and Orbitofrontal Cortex
665 Are Both Required for Model-Based, But Not Model-Free, Reinforcement Learning. *Journal of Neuroscience*, 31(7), 2700–
666 2705. doi: 10.1523/JNEUROSCI.5499-10.2011
- 667 McGinty, V. B., Lardeux, S., Taha, S. A., Kim, J. J., & Nicola, S. M. (2013, jun). Invigoration of reward seeking by cue and
668 proximity encoding in the nucleus accumbens. *Neuron*, 78(5), 910–922. doi: 10.1016/j.neuron.2013.04.010
- 669 Mulder, A. B., Shibata, R., Trullier, O., & Wiener, S. I. (2005, may). Spatially selective reward site responses in tonically active
670 neurons of the nucleus accumbens in behaving rats. *Experimental Brain Research*, 163(1), 32–43. doi: 10.1007/s00221-
671 004-2135-3
- 672 Mulder, A. B., Tabuchi, E., & Wiener, S. I. (2004, apr). Neurons in hippocampal afferent zones of rat striatum parse routes into
673 multi-pace segments during maze navigation. *European Journal of Neuroscience*, 19(7), 1923–1932. doi: 10.1111/j.1460-
674 9568.2004.03301.x
- 675 Nicola, S. M. (2004, apr). Cue-Evoked Firing of Nucleus Accumbens Neurons Encodes Motivational Significance During a

- 676 Discriminative Stimulus Task. *Journal of Neurophysiology*, 91(4), 1840–1865. doi: 10.1152/jn.00657.2003
- 677 Nicola, S. M. (2010). The Flexible Approach Hypothesis: Unification of Effort and Cue-Responding Hypotheses for the Role of
678 Nucleus Accumbens Dopamine in the Activation of Reward-Seeking Behavior. *Journal of Neuroscience*, 30(49), 16585–
679 16600. doi: 10.1523/JNEUROSCI.3958-10.2010
- 680 Niv, Y., Daw, N. D., Joel, D., & Dayan, P. (2007, mar). Tonic dopamine: Opportunity costs and the control of response vigor.
681 *Psychopharmacology*, 191(3), 507–520. doi: 10.1007/s00213-006-0502-4
- 682 Noonan, M. P., Chau, B. K., Rushworth, M. F., & Fellows, L. K. (2017, jul). Contrasting Effects of Medial and Lateral Orbitofrontal
683 Cortex Lesions on Credit Assignment and Decision-Making in Humans. *The Journal of Neuroscience*, 37(29), 7023–7035.
684 doi: 10.1523/JNEUROSCI.0692-17.2017
- 685 Paxinos, G., & Watson, C. (1998). *The Rat Brain in Stereotaxic Coordinates* (4th ed.). San Diego: Academic Press. doi:
686 10.1523/JNEUROSCI.0692-17.2017
- 687 Pennartz, C. M. A. (2004, jul). The Ventral Striatum in Off-Line Processing: Ensemble Reactivation during Sleep and Modulation
688 by Hippocampal Ripples. *Journal of Neuroscience*, 24(29), 6446–6456. doi: 10.1523/JNEUROSCI.0575-04.2004
- 689 Pennartz, C. M. A., Ito, R., Verschure, P., Battaglia, F., & Robbins, T. (2011, oct). The hippocampalstriatal axis in learning,
690 prediction and goal-directed behavior. *Trends in Neurosciences*, 34(10), 548–559. doi: 10.1016/j.tins.2011.08.001
- 691 Peters, J., & Büchel, C. (2009, dec). Overlapping and distinct neural systems code for subjective value during intertemporal and
692 risky decision making. *The Journal of neuroscience : the official journal of the Society for Neuroscience*, 29(50), 15727–34.
693 doi: 10.1523/JNEUROSCI.3489-09.2009
- 694 Rescorla, R. A., & Solomon, R. L. (1967). Two-Process Learning Theory: Relationships Between Pavlovian Conditioning and
695 Instrumental Learning. *Psychological Review*, 74(3), 151–182. doi: 10.1037/h0024475
- 696 Robinson, T. E., & Flagel, S. B. (2009, may). Dissociating the Predictive and Incentive Motivational Properties of
697 Reward-Related Cues Through the Study of Individual Differences. *Biological Psychiatry*, 65(10), 869–873. doi:
698 10.1016/j.biopsych.2008.09.006
- 699 Roesch, M. R., Singh, T., Brown, P. L., Mullins, S. E., & Schoenbaum, G. (2009, oct). Ventral Striatal Neurons Encode the Value
700 of the Chosen Action in Rats Deciding between Differently Delayed or Sized Rewards. *Journal of Neuroscience*, 29(42),
701 13365–13376. doi: 10.1523/JNEUROSCI.2572-09.2009
- 702 Roitman, M. F., Wheeler, R. A., & Carelli, R. M. (2005, feb). Nucleus accumbens neurons are innately tuned for reward-
703 ing and aversive taste stimuli, encode their predictors, and are linked to motor output. *Neuron*, 45(4), 587–597. doi:
704 10.1016/j.neuron.2004.12.055
- 705 Saddoris, M. P., Stamatakis, A., & Carelli, R. M. (2011, jun). Neural correlates of Pavlovian-to-instrumental transfer in the nu-
706 cleus accumbens shell are selectively potentiated following cocaine self-administration. *European Journal of Neuroscience*,
707 33(12), 2274–2287. doi: 10.1111/j.1460-9568.2011.07683.x
- 708 Salamone, J. D., & Correa, M. (2012, nov). The Mysterious Motivational Functions of Mesolimbic Dopamine. *Neuron*, 76(3),

- 470–485. doi: 10.1016/j.neuron.2012.10.021
- Schultz, W. (2016, feb). Dopamine reward prediction error coding. *Dialogues in Clinical Neuroscience*, 18(1), 23–32. doi: 10.1038/nrn.2015.26
- Schultz, W., Apicella, P., Scarnati, E., & Ljungberg, T. (1992, dec). Neuronal activity in monkey ventral striatum related to the expectation of reward. *The Journal of neuroscience : the official journal of the Society for Neuroscience*, 12(12), 4595–610. doi: 10.1523/JNEUROSCI.12-12-04595.1992
- Schultz, W., Dayan, P., & Montague, P. R. (1997, mar). A neural substrate of prediction and reward. *Science*, 275(5306), 1593–1599. doi: 10.1126/science.275.5306.1593
- Sescousse, G., Li, Y., & Dreher, J.-C. (2015, apr). A common currency for the computation of motivational values in the human striatum. *Social Cognitive and Affective Neuroscience*, 10(4), 467–473. doi: 10.1093/scan/nsu074
- Setlow, B., Schoenbaum, G., & Gallagher, M. (2003, may). Neural encoding in ventral striatum during olfactory discrimination learning. *Neuron*, 38(4), 625–636. doi: 10.1016/S0896-6273(03)00264-2
- Shidara, M., Aigner, T. G., & Richmond, B. J. (1998, apr). Neuronal signals in the monkey ventral striatum related to progress through a predictable series of trials. *Journal of Neuroscience*, 18(7), 2613–25. doi: 10.1016/S0896-6273(03)00264-2
- Sjulson, L., Peyrache, A., Cumpelik, A., Cassataro, D., & Buzsáki, G. (2017, may). Cocaine place conditioning strengthens location-specific hippocampal inputs to the nucleus accumbens. *bioRxiv*, 1–10. doi: 10.1101/105890
- Sleezer, B. J., Castagno, M. D., & Hayden, B. Y. (2016, nov). Rule Encoding in Orbitofrontal Cortex and Striatum Guides Selection. *Journal of Neuroscience*, 36(44), 11223–11237. doi: 10.1523/JNEUROSCI.1766-16.2016
- Strait, C. E., Sleezer, B. J., Blanchard, T. C., Azab, H., Castagno, M. D., & Hayden, B. Y. (2016, mar). Neuronal selectivity for spatial positions of offers and choices in five reward regions. *Journal of Neurophysiology*, 115(3), 1098–1111. doi: 10.1152/jn.00325.2015
- Sugam, J. A., Saddoris, M. P., & Carelli, R. M. (2014, may). Nucleus accumbens neurons track behavioral preferences and reward outcomes during risky decision making. *Biological Psychiatry*, 75(10), 807–816. doi: 10.1016/j.biopsych.2013.09.010
- Sutton, R., & Barto, A. (1998). *Reinforcement Learning: An Introduction* (Vol. 9) (No. 5). MIT Press, Cambridge, MA. doi: 10.1109/TNN.1998.712192
- Tabuchi, E. T., Mulder, A. B., & Wiener, S. I. (2000, jan). Position and behavioral modulation of synchronization of hippocampal and accumbens neuronal discharges in freely moving rats. *Hippocampus*, 10(6), 717–728. doi: 10.1002/1098-1063(2000)10:6;717::AID-HIPO1009;3.0.CO;2-3
- Takahashi, Y. K., Langdon, A. J., Niv, Y., & Schoenbaum, G. (2016, jul). Temporal Specificity of Reward Prediction Errors Signaled by Putative Dopamine Neurons in Rat VTA Depends on Ventral Striatum. *Neuron*, 91(1), 182–193. doi: 10.1016/j.neuron.2016.05.015
- Tingley, D., & Buzsáki, G. (2018, jun). Transformation of a Spatial Map across the Hippocampal-Lateral Septal Circuit. *Neuron*, 98(6), 1229–1242.e5. doi: 10.1016/J.NEURON.2018.04.028

- 742 van der Meer, M. A. A., & Redish, A. D. (2011). Theta Phase Precession in Rat Ventral Striatum Links Place and Reward
743 Information. *Journal of Neuroscience*, 31(8), 2843–2854. doi: 10.1523/JNEUROSCI.4869-10.2011
- 744 West, E. A., & Carelli, R. M. (2016, jan). Nucleus Accumbens Core and Shell Differentially Encode Reward-Associated Cues after
745 Reinforcer Devaluation. *Journal of Neuroscience*, 36(4), 1128–1139. doi: 10.1523/JNEUROSCI.2976-15.2016
- 746 Wiener, S. I., Shibata, R., Tabuchi, E., Trullier, O., Albertin, S. V., & Mulder, A. B. (2003, oct). Spatial and behavioral correlates
747 in nucleus accumbens neurons in zones receiving hippocampal or prefrontal cortical inputs. *International Congress Series*,
748 1250(C), 275–292. doi: 10.1016/S0531-5131(03)00978-6
- 749 Yun, I. A., Wakabayashi, K. T., Fields, H. L., & Nicola, S. M. (2004). The Ventral Tegmental Area Is Required for the Behavioral
750 and Nucleus Accumbens Neuronal Firing Responses to Incentive Cues. *Journal of Neuroscience*, 24(12), 2923–2933. doi:
751 10.1523/JNEUROSCI.5282-03.2004